# SEISMIC PROCESSING OF U.S. EAST COAST DATA

## A DISSERTATION

***Submitted in partial fulfilment of the***

***Requirements for the award of the degree***

***Of***

**INTEGRATED MASTER OF TECHNOLOGY**

***In***

**GEOPHYSICAL TECHNOLOGY**

***By***

**SUJAY PRAKASH SULE**


**DEPARTMENT OF EARTH SCIENCES**

**INDIAN INSTITUTE OF TECHNOLOGY ROORKEE**

**ROORKEE -247667(INDIA)**

**MAY, 2019**

# CANDIDATE'S DECLARATION

I hereby declare that the work which is has been presented in this dissertation entitled,

"**Seismic Processing of U.S. East Coast data**" in partial fulfillment of the requirements for the award of the degree of **INTEGRATED MASTER OF TECHNOLOGY** in **GEOPHYSICAL TECHNOLOGY**, submitted in the Department of Earth Sciences, Indian Institute of technology, Roorkee, is an authentic record of my own work carried out under the guidance of **Prof. Sagarika Mukhopadhyay**, Department of Earth Sciences, IIT Roorkee, during the period of January 2019 to May 2019.

The matter embodied in this dissertation has not been submitted by me for the award of any other degree or diploma of this institute or any other university/institute.

Date: May, 2019
Place: Roorkee

Sujay Prakash Sule,
Integrated M.Tech Fifth year,
Geophysical Technology,
Department of Earth Sciences,
IIT Roorkee,
Roorkee (247667), India.

# CERTIFICATE

This is to certify the work presented in this thesis entitled "**Seismic Processing of U.S. East Coast data**" submitted by Mr. Sujay Prakash Sule to Indian Institute of Technology, Roorkee, India, in partial fulfillment of the requirements for the award of the degree of **INTEGRATED MASTER OF TECHNOLOGY in GEOPHYSICAL TECHNOLOGY** is a record of bona fide original work carried out by his under our supervision during the academic year 2018- 2019.

**Dr. Sagarika Mukhopadhyay**
**Professor, Department of Earth Sciences**
**Indian Institute of Technology Roorkee, Roorkee-247667, India**

# ACKNOWLEDGEMENT

*First and foremost, I would like to express my heartfelt gratitude to my thesis advisor,* ***Dr. (Mrs.) S. Mukhopadhyay, Professor, Indian Institute of Technology, Roorkee*** *for her continuous support and encouragement while also allowing me the room to work in my own way. She went the extra mile in making sure that I had all the necessary facilities needed for completing this work. It was truly an honour and a great learning experience for me to get to work under her.*

*I am highly obliged to* ***Prof. Sunil Bajpai, Head of the Department, Department of Earth Sciences, IIT Roorkee*** *and* ***Dr. Anand Joshi****, O.C. Dissertation, for providing the administrative support required for the completion of this work.*

*I am especially indebted to* ***Sr. Geophysicist, Mr. Subhra Pratim Das, ONGC*** *for sharing expertise and offering the much needed insight in tackling various problems that I had encountered during different stages of processing.*

*I am also very thankful and deeply indebted to all peers and colleagues who have helped with my work. Each one of them has inspired me to work harder for this thesis. Also, I am thankful to all those who have helped me directly or indirectly to make this dissertation work successful.*

*A special mention to* ***U.S. Geological Survey*** *for making this data set available for academic and research purpose.*

# ABSTRACT

*Seismic method is the mainstay of geophysical exploration. The main reasons for its success include its accuracy, the depth of penetration and the ability to generate high resolution image of subsurface, while being relatively economical at the same time. The present study uses the technique to study the subsurface structure and the geometry of reflectors across the eastern edge of North American shelf off the coast of U.S. The continental shelves are hotbeds for oil and gas exploration; and hence, here we would try to identify possible traps within region.*

*Our area of interest includes two large sedimentary basins that underlie the said region, the Carolina trough and the Blake Plateau basin. Each of them marks a distinct geological province. The Carolina trough is dominated by a terrigenous-clastic depositional regime, whereas the Blake Plateau is transitional into a carbonate-platform depositional regime.*

*Three profiles (lines 30, 31, and 32) were chosen such that they run across the shelf which would allow us to study the cross sectional view of the region. The obtained dataset is without geometry information and is heavily contaminated by reverberations and back-scattered noise. We first start by merging geometry information, editing out bad traces and correcting for geometric spreading, collectively termed as pre-processing. Then a series of filters, including deconvolution, dip filtering and radon transform, were applied to attenuate coherent noise. Deconvolution would also help in increasing the temporal resolution. Velocity analysis was performed and number of velocity models tested; and the best suiting one was used to migrate and finally stack the dataset. In the end, some final conditioning was done to further enhance the reflectors.*

*We have observed three major reflectors in all the studied profiles, with many minor ones present in between. A major fault can be seen in the seismic section of line 32, which may favour formation of some minor structural traps. An amplitude shadow resembling gas chimney effect is also observed, which points toward a possible gas deposit in the region. The on-laps and off-laps evident in all three profiles are indicative sea-level changes.*

# TABLE OF CONTENTS

# TABLE OF FIGURES

# 1. INTRODUCTION

Seismic method is one the most widely used methods of geophysical exploration, given its accuracy and great depth of penetration as well as the ability to construct high resolution image of subsurface. The technique generates seismic waves and records the amount of time they take to travel from a source to a series of geophones/hydrophones. The recorded travel times when combined with the knowledge of wave-velocity, one can easily estimate the distance traversed and the path taken. Geometry and structural information is mostly extracted from the reflected waves & head-waves (Fig.1.1.1). For both, the attitude of beds and the physical properties of formation, such as density & elastic moduli, determine the propagation velocity and thus, the travel times of the seismic waves.

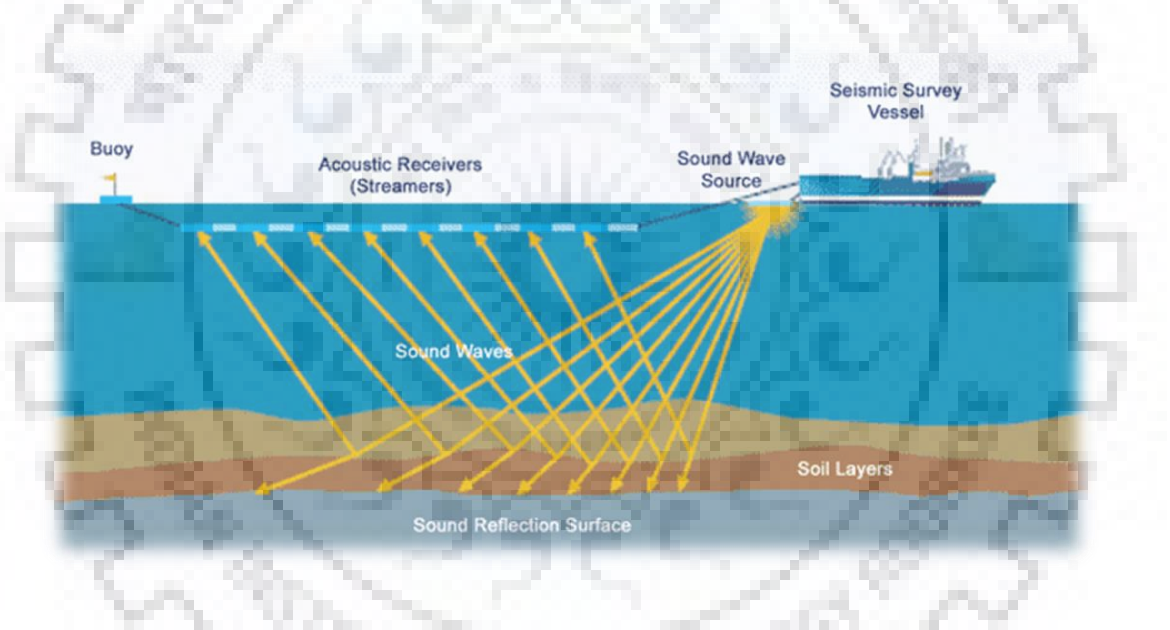


**Figure 1.1.1: Marine seismic survey (Source - https://bit.ly/2vUntsW).**

The seismic method has three principal applications: (Yilmaz, 2001):

- Engineering seismology for determining the near surface geology for engineering studies, and coal & mineral exploration up to a depth of up to 1 km.
- Exploration seismology for hydrocarbon exploration and development up to a depth of up to 10 km.
- Earthquake seismology for investigating the internal structure of earth and source characteristics of earthquakes using records of earthquakes.

# 1.1. DATA ACQUISITION

The present work will apply reflection seismic method in a marine setting to delineate the structural setting across the eastern edge of North American shelf. This method basically comprises of 3 steps:

- **Data Acquisition**
- **Data Processing**
- **Data Interpretation**

The basic aim of data acquisition is to record a signal having high signal-to-noise ratio and a broader bandwidth for better resolution to fulfil the geological objectives. Seismic acquisition system consists of the following elements:

- Energy source
- Energy receiving unit
- Digital recording system

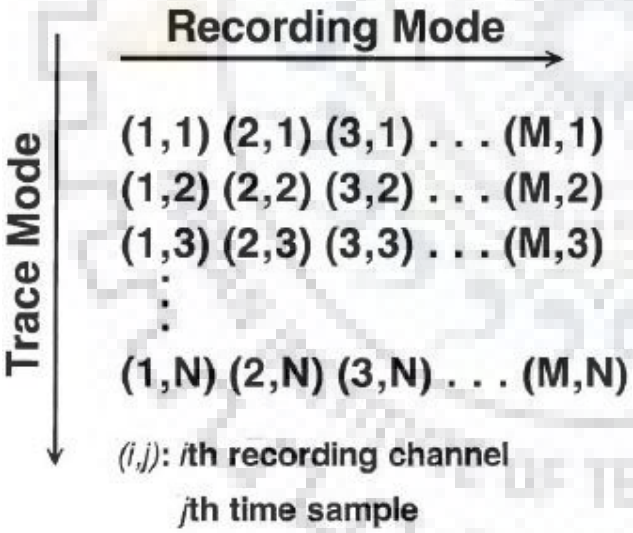


**Figure 1.1.2: Sample data matrix showing difference between multiplexed recording mode and demultiplexed trace mode (Yilmaz, 2001).**

The most common marine seismic sources are air-gun, steam-gun and hydro-gun, which generate acoustic waves by releasing pressurised air, steam or water. They are generally used in arrays in order to amplify the signal and minimize the source related incoherent noise e.g. bubble oscillation. The hydrophones are generally based on piezoelectric transducers which convert pressure-changes, a mechanical input into an electrical output.

Depending on the purpose of the survey, the source-receiver geometry is decided. A survey vessel tows the streamer(s) made up of source and receiver arrays (Fig.1.1.1). The source moves along the seismic line and generates seismic waves at regular intervals. As the shot goes off, signals are recorded on each hydrophone for a certain length of time, producing a series of traces. The recorded traces from each shot are relayed to the recording seismic vessel through an assembly of buoyant electric cables.

Seismic data is acquired in multiplexed format i.e. in a time-ordered format and needs to be demultiplexed i.e. converted into a receiver-ordered format before processing begins (Fig.1.1.2). Many modern instruments do this in field. The most commonly used format for seismic processing, SEG-Y is trace-sequential format.

# 1.2. DATA PROCESSING

Seismic data processing is a sequence of operations to transform the recorded raw data to create an image of subsurface that is interpretable by a competent person. The aim of data processing is to eliminate subtle noises in the data and to estimate subsurface geometry using primary reflections. Subtle noises in the data can be random and coherent noises such as reverberations, multiple reflections (multiples), ground rolls, linear noise related to guided waves and point scatters. The three important steps of data processing are (Yilmaz, 2001):

- **Deconvolution:** Performed along time axis (Fig.1.2.1) to increase temporal resolution by suppressing reverberations and spiking the source wavelet.
- **CMP stacking:** Compresses offset axis (Fig.1.2.1) by reducing common-midpoint (CMP) gathers to zero offset section while increases signal-noise ratio in the process.
- **Migration:** Moves dipping seismic events to their true locations and collapses diffraction hyperbolas, and as a result, increases the lateral resolution.

Secondary processes are applied to condition the data and increase the robustness of the above mentioned methods (Fig.1.2.2). Deconvolution increases temporal resolution but it also introduces unwanted artefacts. An appropriate bandpass filter needs to be applied to check this problem.

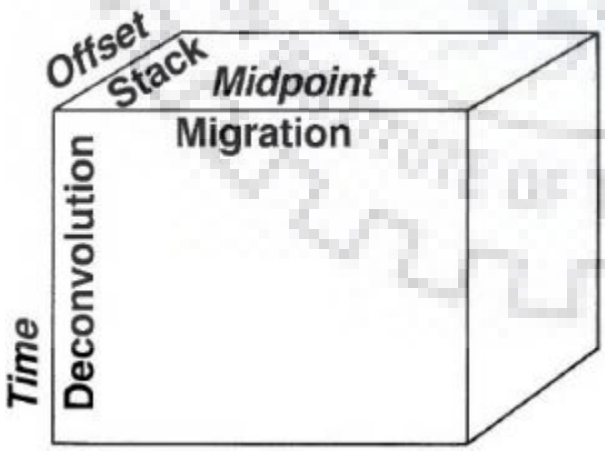


**Figure 1.2.1: Seismic data volume expressed as processing coordinates: midpoint-offset-time (Yilmaz, 2001).**

Stacking greatly attenuates coherent (multiples and guided waves) and incoherent noise. Since multiples have larger moveouts they remain under-corrected after NMO

correction is applied, and as a result get attenuated after stacking. However, it is important to ensure that proper stacking velocities are used.

Techniques such as $f - k$ filtering (dip filtering), slant-stacking, radon filtering are used to supress coherent noise such as ground-roll, guided waves and direct arrivals. Velocity analysis can be performed after each of these stages to get better estimates of stacking velocity thus, improving the stacking output.

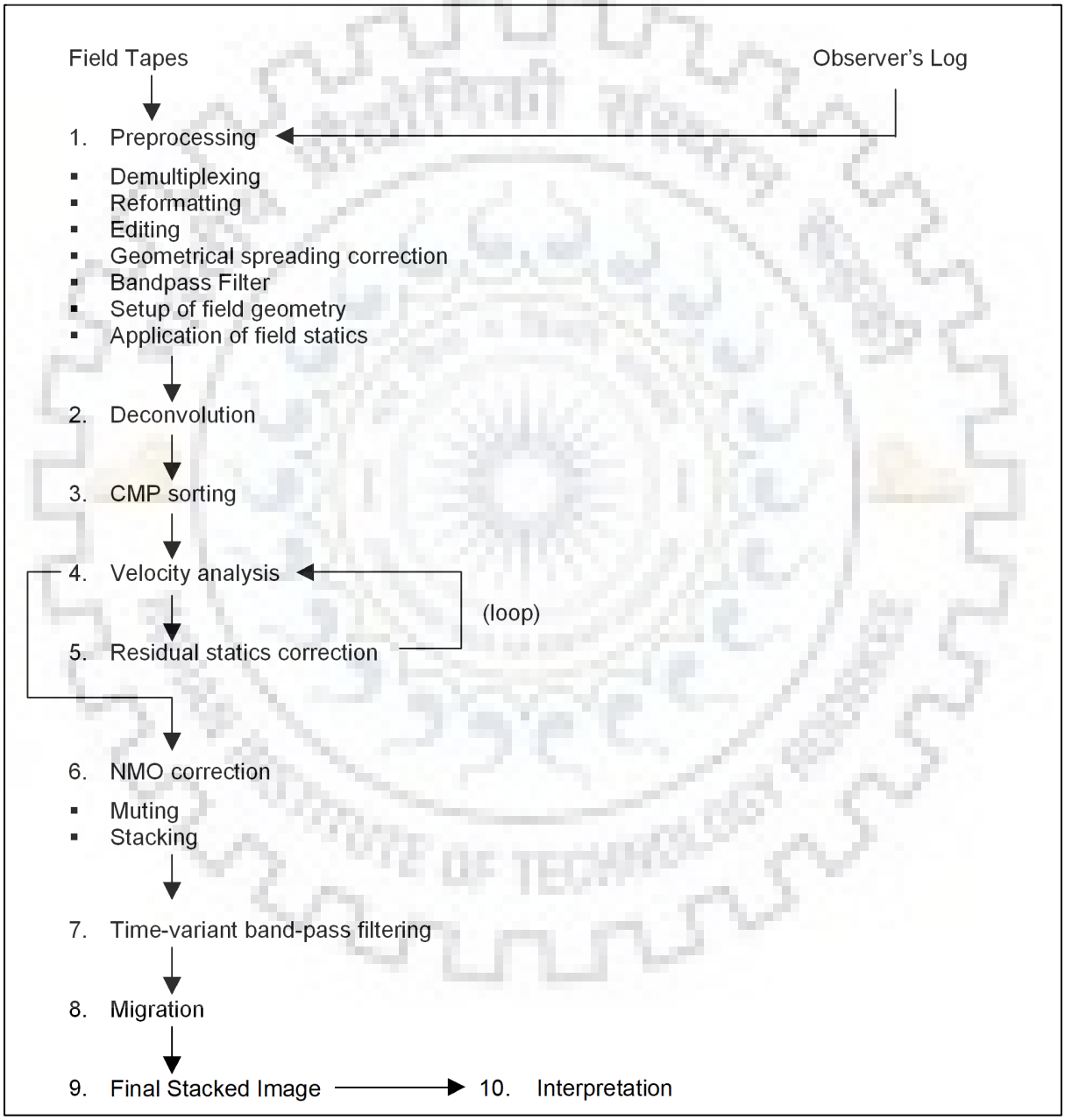


**Figure 1.2.2: Flow-chart detailing basic processing steps (Yilmaz, 2001).**

Migration is an imaging process based on the wave equation. It requires the data to be noise free. In case of 2D dataset, migration can't account for out-of-the-plane reflections and they remain uncorrected. Factors that influence the migration results are (Yilmaz, 2001; Yilmaz, 1979; Benson and Stolt, 1986):

- Noise (mainly coherent noise)
- Spatial sampling (in the presence of steep dips, aliasing can be a problem)
- Migration aperture (related to the horizontal displacement of the reflection point)
- Amplitude anomalies (spikes, noise outbursts, truncated traces)
- Input data (2D or 3D data)
- Migration strategies (time or depth, post or pre-stack)

# 1.3. DATA INTERPRETATION

Interpretation is the art of determining geology at a given depth from the processed record of seismic data. Despite the advances in acquisition and processing techniques, it is still required of the interpreter to draw from his understanding of geology and the dataset to identify the correct and most plausible interpretation from the many other possible solutions. The process of interpretation can be divided into three inter-related categories:

- **Structural interpretation:** Here we try to reconstruct the structural maps of the subsurface from the recorded arrival times.
- **Stratigraphic interpretation:** Here we try to compare the pattern of observed reflections with a known model of cyclic deposition with the aim of establishing a chronostratigraphic relation.
- **Lithologic interpretation:** Here we try to infer the changes in rock properties such as porosity, fracture intensity, pore fluid, lithology, etc. from seismic data.

Structural interpretation will be carried out in this work. Much more could be inferred by studying the seismic attributes such as instantaneous amplitude, phase, frequency, polarity, etc., as they could provide direct indication of hydrocarbons present. Bright-spot, presence of amplitude and frequency shadow, flat-spot, gas chimney effect, etc. are some direct indicators of hydrocarbons.

# 2. STUDY AREA

## 2.1. LOCATION

Study area is located along the eastern margin of North American shelf and includes lines 30, 31, and 32 (highlighted in Fig.2.1.1).

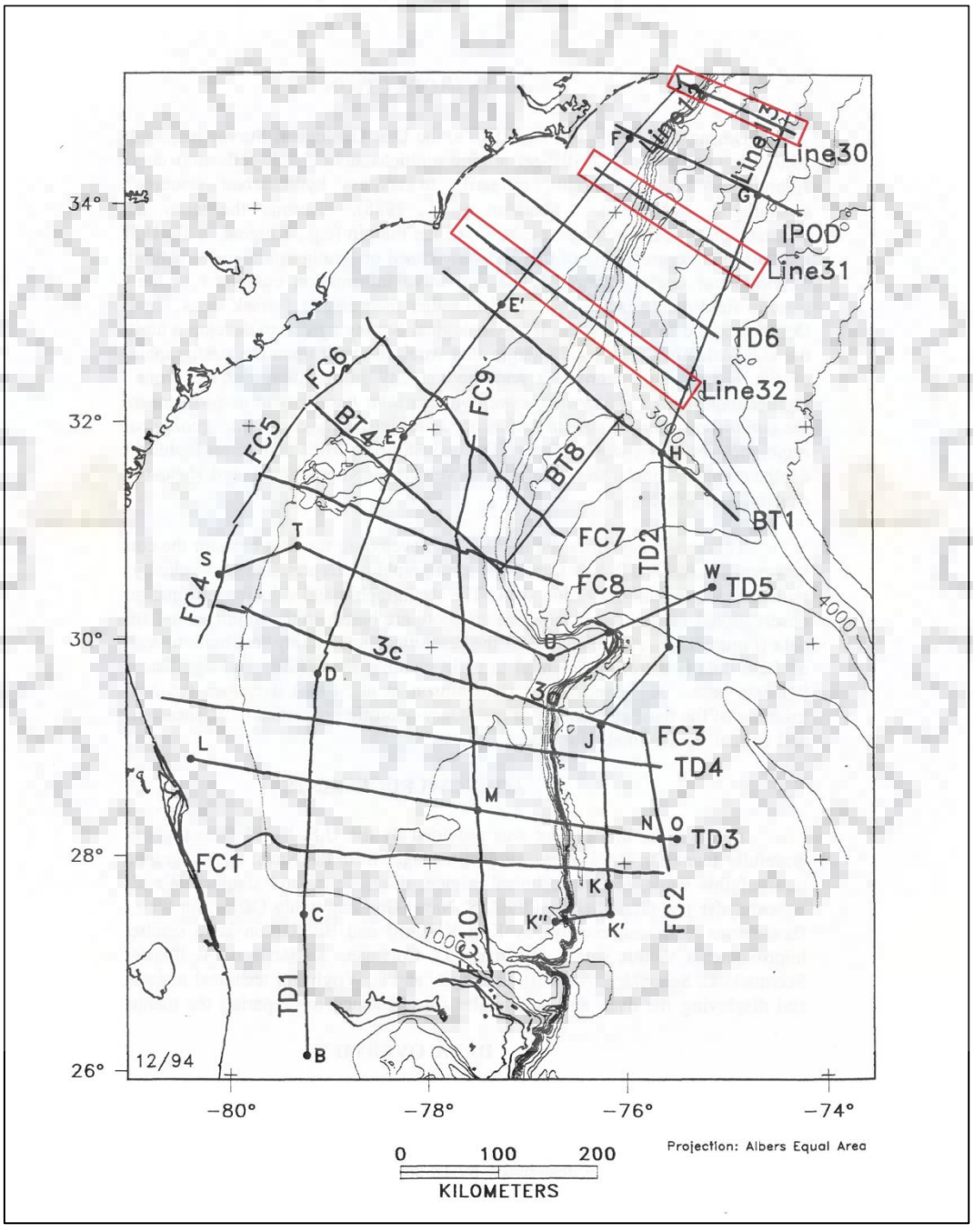


**Figure 2.1.1: The coastal plain, continental shelf, slope and rise of the U.S. East Coast (NOS, 1986).**

# 2.2. TECTONIC SETTING

South of Carolina trough, there are two large sedimentary basins underlying the U.S. continental margin, Cape Hatteras, and the Blake Plateau basin (Fig.2.2.1); each marks a distinct geological province. These basins were formed as the continental margin gradually evolved following the separation of Africa and North America in Middle Jurassic time. The Florida and Carolina platforms form the landward sides of these basins, respectively. The Carolina trough and the Blake Plateau basin have the greatest contrasts of any of the large offshore Atlantic basins (Poag, 1991).

The Carolina trough is the narrowest and most linear of the basins and the Blake Plateau is the widest and most equidimensional. The Carolina trough is underlain by narrow rift basins and extensive salt deposits (Hutchinson et al., 1983; Dillon et al., 1983) whereas rifting in the Blake Plateau occurred over a much wider zone and no salt deposits are known (Dillon et al., 1988). The Carolina trough is dominated by a terrigenous-clastic depositional regime; the Blake Plateau is transitional into a carbonate-platform depositional regime best developed in the Bahamas to the south.

The continent-ocean transition is well marked by a prominent magnetic anomaly in the Carolina trough, the East Coast Magnetic Anomaly. No similar geophysical marker exists along the Blake Plateau basin, and the continent-ocean transition is presumed to underlie the Blake Escarpment (Dillon et al., 1988).

The break-up history of the Carolina trough and Blake Plateau regions also differed significantly. Sea-floor spreading was initiated in the Carolina trough by 175 Ma, but was delayed by about 4 my in the Blake Plateau until 171 Ma (Dillon et al., 1988). Within a million years, at 170 Ma, a spreading-centre jump occurred at the position of the Blake Spur magnetic anomaly. Numerous oceanic fracture zones project into the continental margin from oceanic crust (Fig.2.2.1); the largest is the Blake Spur fracture zone, which separates the Carolina trough from the Blake Plateau basin (Klitgord et al., 1979).

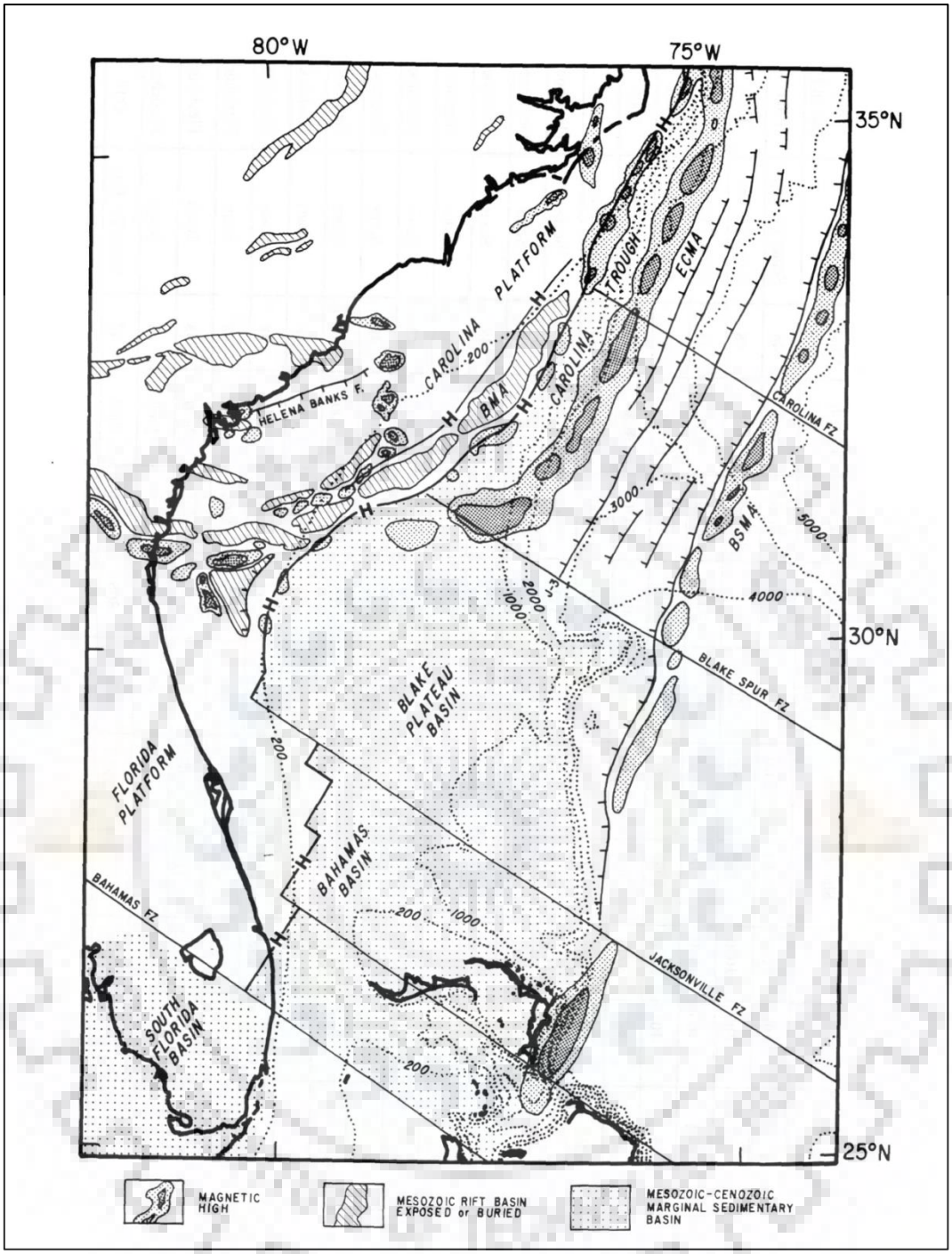


**Figure 2.2.1: Simplified tectonic map of the continental margin (NOS, 1986).**

# 2.3. STRATIGRAPHY

No dated samples older than Early Cretaceous have been recovered from this part of the continental margin in either shallow or deep water (Sheridan et al., 1979; Dillon et al., 1985); therefore, the geologic interpretation of the rift and early post-rift formation of the margin is based on seismic character, inference, and comparison with the continental margin to the north.

The post-rift sedimentary history of the Blake Plateau began in the Jurassic with widespread carbonate deposition and reef building along the eastern portion of the margin. The Blake Plateau did not exist as a deep water environment: the region was characterized by shallow-water, carbonate deposition. Much of this carbonate deposits lead to formation of a giant Jurassic reef system that extended from the Bahamas to Georges Bank (Poag, 1991). Anhydrite deposits of Jurassic age are recorded in wells from the Bahamas (Tator et al., 1975). Deposition is more terrigenous on the western side of the region.

During the Early Cretaceous, carbonate deposition slowed and reef development ended from north to south. By the end of Cretaceous time, rising sea level and the resulting subsidence produced the deep water Blake Plateau, which then became a region starved of sedimentation, characterized by authigenic and biogenic deposition (Dillon et al., 1988).

Cenozoic time has been dominated by erosional processes and the eventual development of widespread regional unconformities. It was during this time that the ocean currents such as the Suwanee, Gulf Stream, and Deep Western Atlantic Boundary currents were initiated. Changes in sea level have caused the Gulf Stream to migrate across the Blake Plateau, affecting sediment deposition patterns (Dillon et al., 1988).

One of the most notable features that have modified the stratigraphy through time is salt migration into diapirs in the Carolina trough. Evaporites were among the earliest deposits in late rift and early post-rift formation of the margin, and these deposits have mobilized upward through the overlying sediments to form a linear chain of diapirs (Dillon et al., 1983). Few of the diapirs reach the sea floor and they appear to

be confined to the seaward edge of the Carolina trough. None are known in the Blake Plateau basin.

Faults have also modified the region. Growth faults are associated with salt diapirism near the shelf edge (Dillon et al., 1983). Large normal faults are interpreted near the edge of the Blake Escarpment on several profiles (Hutchinson et al., 1995). Extensive mapping in the inner shelf has revealed the existence of young neo-tectonic faults (Behrendt et al., 1983) which could be related to ongoing low-level seismicity in the south-eastern United States (Behrendt et al., 1986).

# 3. METHODOLOGY

Here we would discuss the complete processing workflow for transforming raw seismic data into seismic cross-section of subsurface through a series of operations. But before starting, it is important to take a note of events that occur on field when data is recorded. Both the strategies used for processing data and the results produced, are heavily affected by field acquisition parameters and the conditions prevailing on field when acquisition is carried out.

Observers on field keep a track of such events by noting down everything that could affect the quality of data, which includes parameters like tow depths, conditions at sea, source configuration, etc. All of this information is documented in Observer's Log. Some important things that one must check in Observer's Log are (Yilmaz, 1979):

- Shooting geometry: Total number of active channels, the distance between centres of first receiver-group and source-array (i.e. the near trace offset), the receiver & shot intervals, and the far trace offset.
- Field file identification numbers (FFIDs): Usually same as shot-point numbers. In case of missing/dropped shots we may need to renumber the shot-points.
- Gun delay: Generally the systems begin data recording some time before the airgun goes off, introducing a delay that needs to be removed.
- Bad traces or files as a result of some noise.
- Sample rate and record length.
- Channel nearest/farthest from source.
- Shot-point numbers (incrementing/decrementing)
- Aliasing filters applied which recording, etc.

The Observer's Log is a key piece of "metadata" and hence, it is extremely useful to the processor. Table 3.1 lists some acquisition parameters as given in Observer's log (Fig.3.1.1):

| | |
|---|---|
| **Spread type:** | **End-on** |
| **No. of shots:** | **1794** |
| **Near offset:** | **540 meters** |
| **Shot interval:** | **50 meters** |
| **Receiver interval:** | **75 metres** |
| **Sampling interval:** | **4 milliseconds** |
| **Record length:** | **12 seconds** |
| **No. of active channels:** | **48** |
| **Channel no. closest to shot:** | **48** |
| **Nominal foldage:** | **48** |
| **Gun delay:** | **51 milliseconds** |
| **Gun depth:** | **21 metres** |
| **Filter applied:** | **Bandpass (8-62 Hz)** |

**Table 3.1: List of acquisition parameters**

After analysing the information available in Observer's logs we can move on to processing stage. Seismic processing, broadly divided into 3 parts, consists of following steps:

- Pre-processing
    - Demultiplexing/Reformatting
    - Updating geometry information
    - Editing and Amplitude scaling
    - Geometrical Spreading Correction
    - Bandpass filtering and muting
    - Application of field statics
- Processing
    - Deconvolution
    - Attenuating linear noise
    - CDP sorting and Velocity Analysis
    - RMS volume generation
    - Pre-Stack Time Migration (PSTM)
    - Stacking

- Post-processing
    - Time-Variant Band-pass Filtering
    - Deconvolution after stack
    - Signal Enhancement

This is only a basic outline for seismic processing. Some additional processing steps may be needed or some of the above mentioned steps may not be applied depending on the dataset. These steps are discussed in further detail along with their practical application on seismic profile “Line 31” using Paradigm software suite.

# 3.1. PRE-PROCESSING

Raw seismic data is a series of traces with no navigation and geometry information. It is plagued by a number of problems such as missing shots, bad/noisy traces or traces having their polarity reversed. In addition there might be some auxiliary traces present that must be removed. Most of the information required for making these corrections is contained in Observer's logs, thus, making them quite handy for pre-processing.

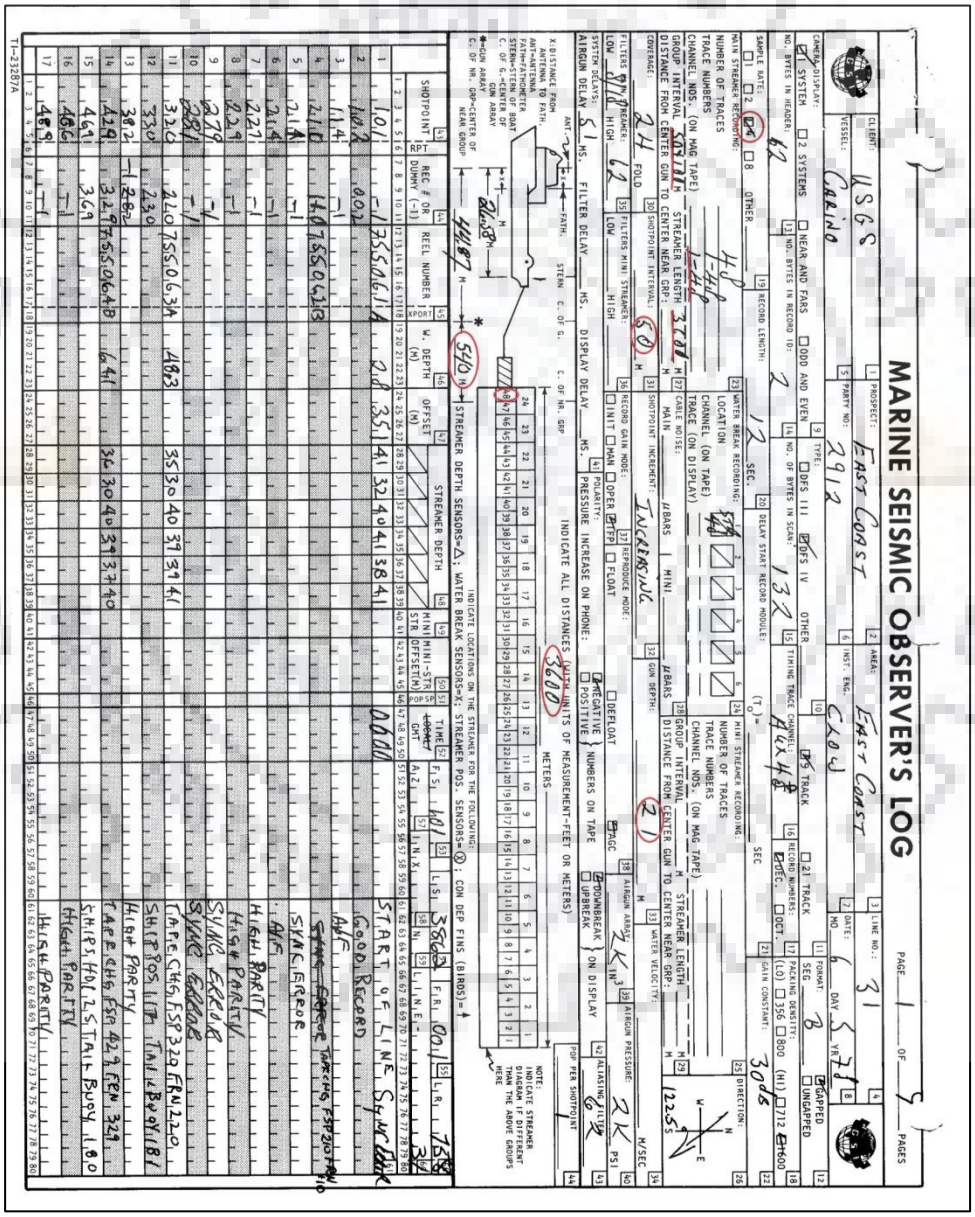


**Figure 3.1.1: A page form Observer's log of line 31 detailing the acquisition parameters of the survey.**

## 3.1.1. DATA LOADING

We start by loading data into the system. Profile data downloaded from USGS is written in SEG-Y format. The dataset can be imported using the option of “SEG-Y Import and Create New Survey” available in Epos Utilities of Paradigm. A dialogue box opens prompting to select the measurement-system (Fig.3.1.2) before asking for the location of data to be loaded (Fig.3.1.3) and to create a survey line.

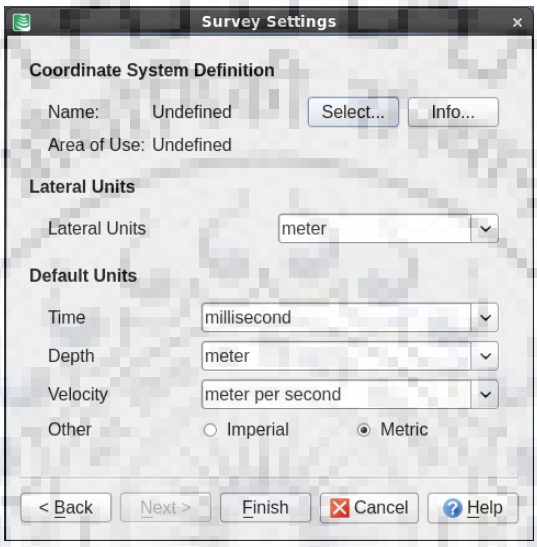


**Figure 3.1.2: Dialogue box asking measurement units to use in survey (Source - Paradigm).**

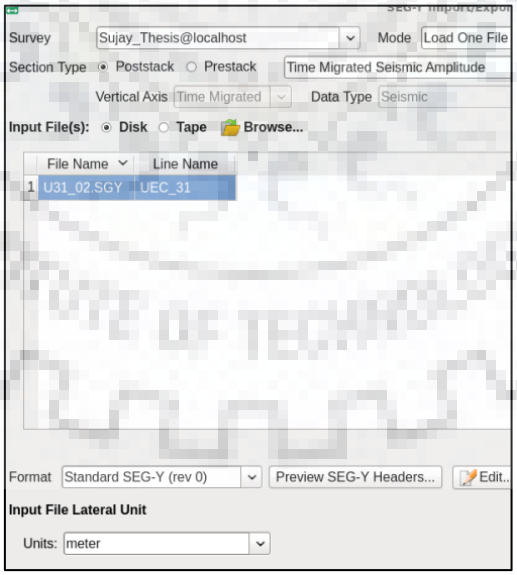


**Figure 3.1.3: Dialogue box asking for fata location before creating survey (Source - Paradigm).**

Paradigm can read any trace-sequential tape format such as SEG-Y and reformat it to the internal format, called Paradigm Dataset (PDS) format, required by all other

program before storing it on disk. It is capable of reading selected ensembles of data from among those on a tape. It can also read a single set of data from an archived tape on which several reels of data have been stored.

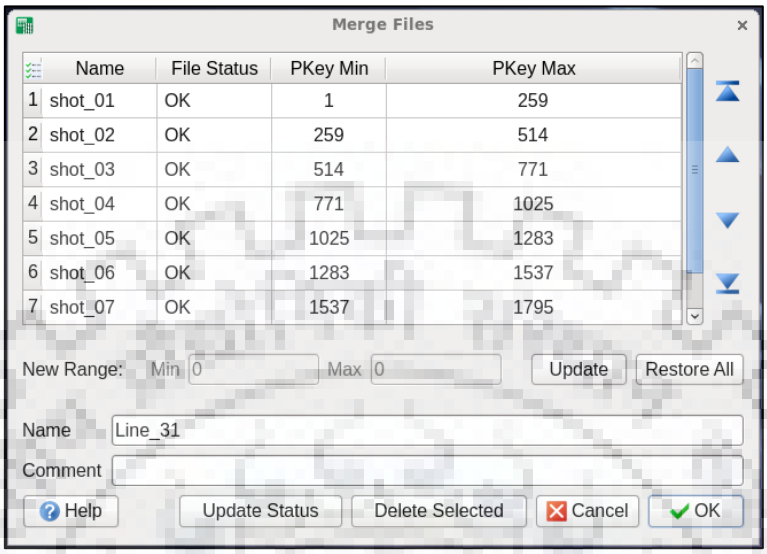


**Figure 3.1.4: Dialogue box showing merging of a fragmented dataset under a single file "Line 31" (Source – Paradigm).**

Data of line 31 was recorded in seven different volumes (as shown in Fig.3.1.4). Each volume is loaded separately and labelled accordingly. After this, all of these volumes were merged into a single file labelled "Line_31" (Fig.3.1.4). To ensure that every file was loaded properly, we compared the minimum and maximum values of primary-key (Fig.3.1.4) i.e. field file identification numbers (FFIDs) of the loaded dataset with the information from Observer's log and found everything to be in place

## 3.1.2. GEOMETRY MERGING

As mentioned before, raw does not come with geometry information loaded and only has field file identification numbers (FFID) and sequence numbers to distinguish between individual shot-gathers and traces respectively.

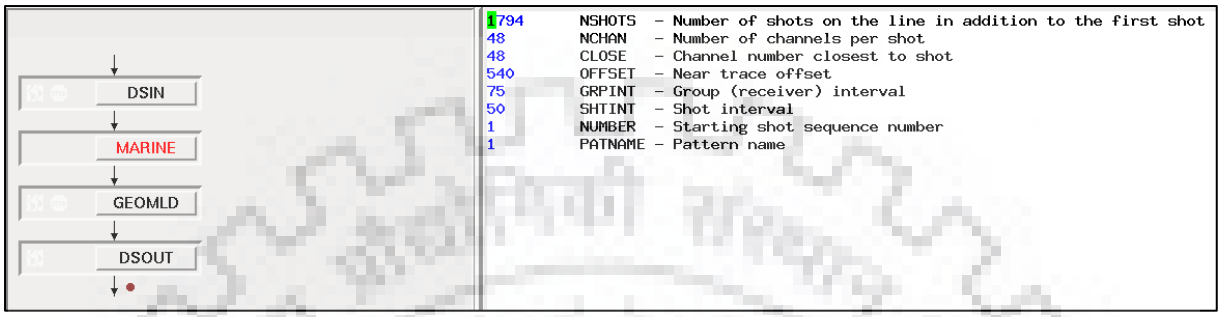


**Figure 3.1.5: Workflow of geometry merging for marine data, showing the acquisition parameters used for creating the geometry spreadsheet in "MARINE" module (Source - Paradigm).**

The "MARINE" module uses acquisition parameters (Table 3.1 and Fig.3.1.5) as input to generate a 2D marine geometry spreadsheet. The information from this spreadsheet is then assigned to the dataset by using "GEOMLD" module (Fig.3.1.6). This process must precede any step requiring offset information.

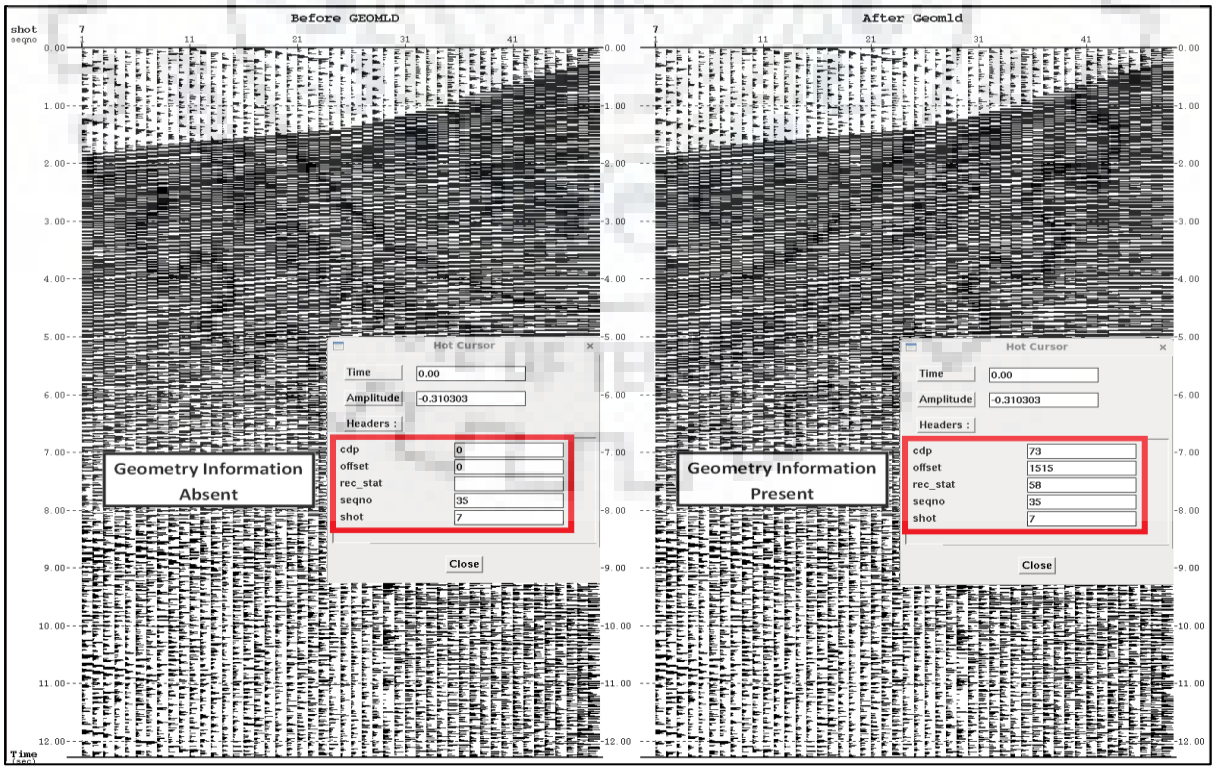


**Figure 3.1.6: Result of geometry merging (right) showing geometry information that is added to raw data.**

## 3.1.3. TRACE EDITING

The shot gathers may contain some bad traces which include the traces that are too noisy or traces have consistently low amplitudes or traces with reversed polarity. This might happen as a result of poor coupling or faulty components. Such traces are edited to remove/alter bad traces using “EDIT” module in following ways (Fig.3.1.7):

- Reducing trace amplitude to zero (set parameter “OPER” to “KILL”)
- Drop the trace from processing (set parameter “OPER” to “OMIT”)
- Reverse the amplitude polarity of trace (set value of parameter “SKEY” as negative, nullifying OMIT/KILL)

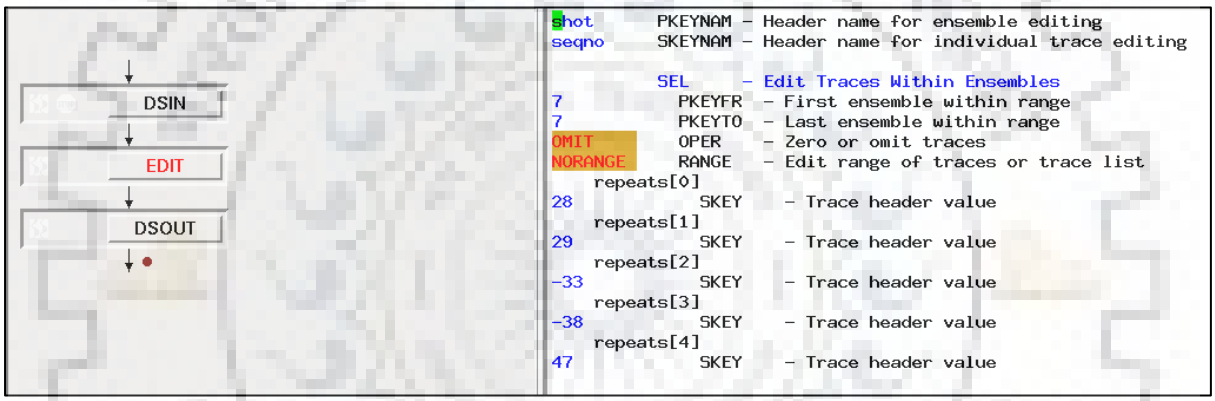


**Figure 3.1.7: Workflow of trace-editing showing sequence number of traces that were omitted or had their polarity changed. This changes were applied to all ensembles i.e. shot-gathers (Source - Paradigm).**

It is to be noted that “EDIT” module applies these changes to all relevant traces of every shot-gather. But if such changes are needed in a single shot-gather, we could opt for interactive editing by using “IEDIT” module in pause mode. The commands that are available here include:

- Omit: To completely drop a trace.
- Zero: To make the amplitude of the selected trace zero.
- Zero Beg: To trim the trace from top to the point selected.
- Zero End: To trim a trace from a point to the end of the trace.
- Reverse: To reverse the polarity of a trace.

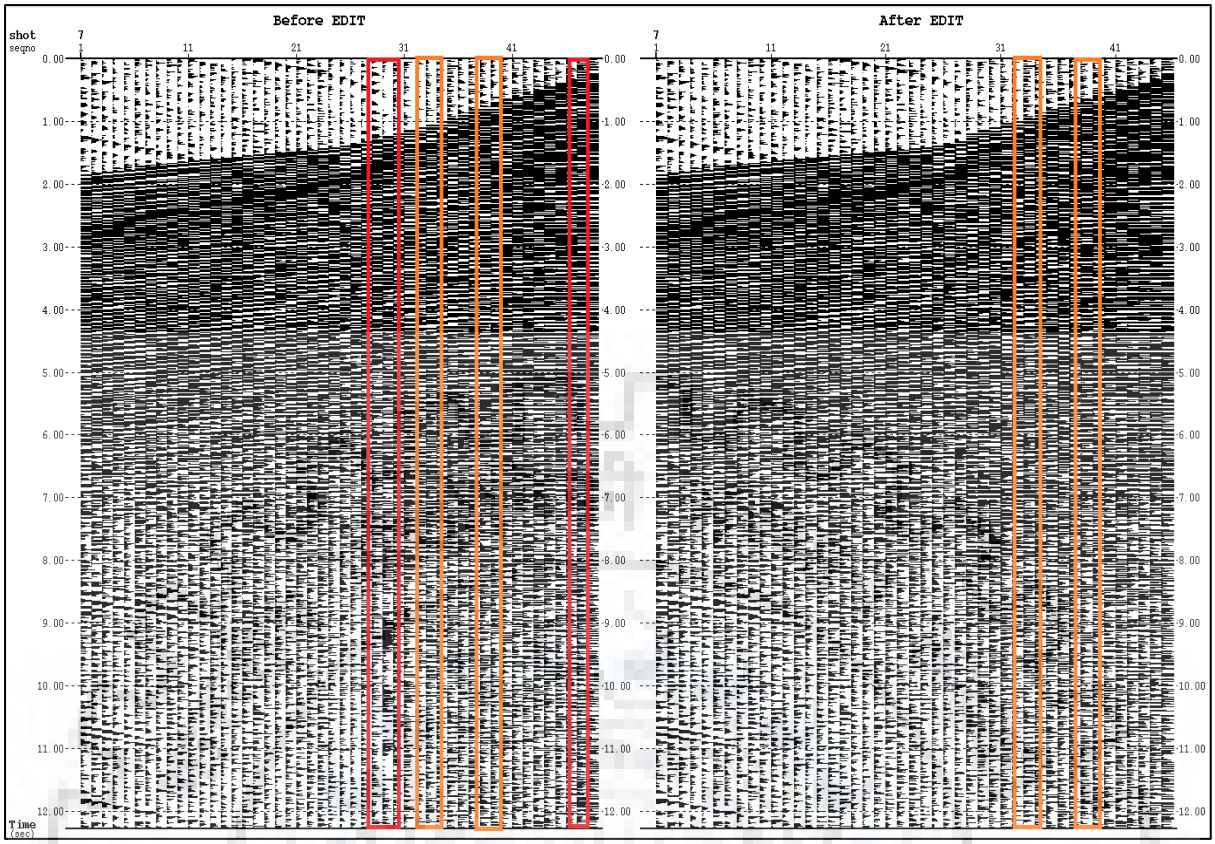


**Figure 3.1.8: Result of trace-editing (right) showing traces that were omitted in red boxes and those which had their polarity reversed in orange boxes.**

## 3.1.4. AMPLITUDE RECOVERY

Seismic record represents a wave-field generated by a point source, which conceptually must be spherical in shape. In homogenous medium the decay in energy of this wave-field is inversely proportional to the square of distance travelled, which means amplitude decay must be inversely proportional to distance travelled. In real earth situation, velocity increases with depth causing further divergence. To correct this, we must apply an artificial gain so that the deep reflectors become clearer.

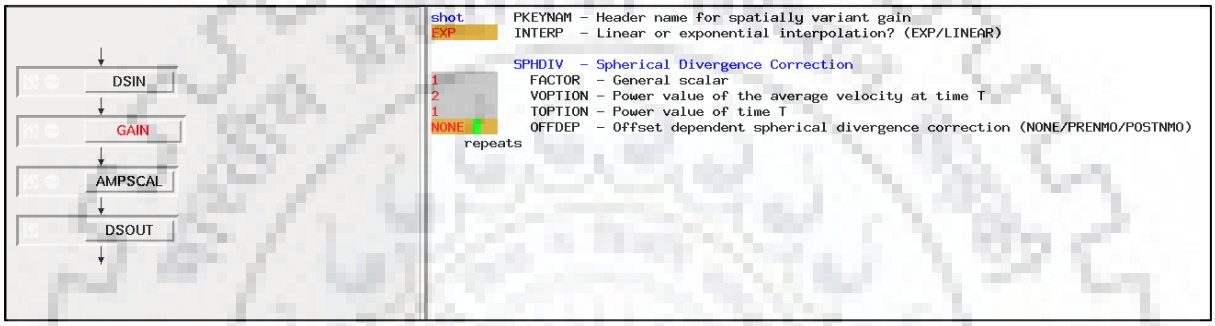


**Figure 3.1.9: Workflow of amplitude recovery and trace balancing, showing the value of parameters used for applying spherical divergence correction (Source - Paradigm).**

Amplitude recovery is performed using "GAIN" module (Fig.3.1.9). It helps in balancing of seismic trace amplitude by applying a time-variant exponential or linear scalar to a set of data. Options are also available to remove the effect of offset independent or dependent spherical divergence.

The "SPHDIV" option is used (Fig.3.1.9) for spherical divergence corrections in order to account for decrease in amplitude of seismic wave due to the geometrical spreading of the wave front. The decrease in amplitude occurs as the distance to the signal from the energy source increases.

It works by multiplying each sample of every trace by the length of radius of the spherical wave emanating from the shot at the time of the sample. The value of this radius is given by a scalar expressed as function (eq. 3.1.4.1) of travel-time (T):

$$SCALAR\ (T) = \frac{\left(V_{rms}(T)^{VOPTION}\right) \times \left(T^{TOPTION}\right)}{(V_o \times SCMAX)} \qquad (3.1.4.1)$$

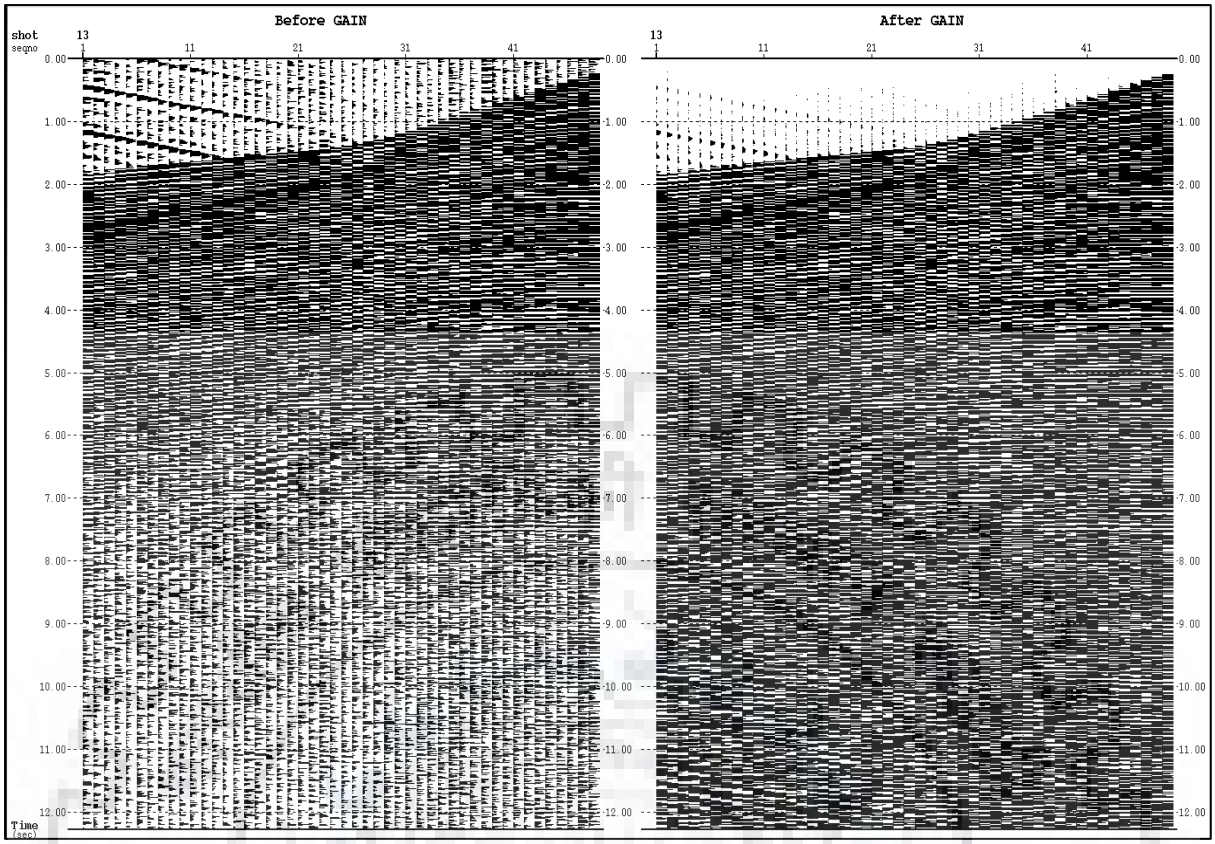


**Figure 3.1.10: Before (left) and after (right) amplitude recovery.**

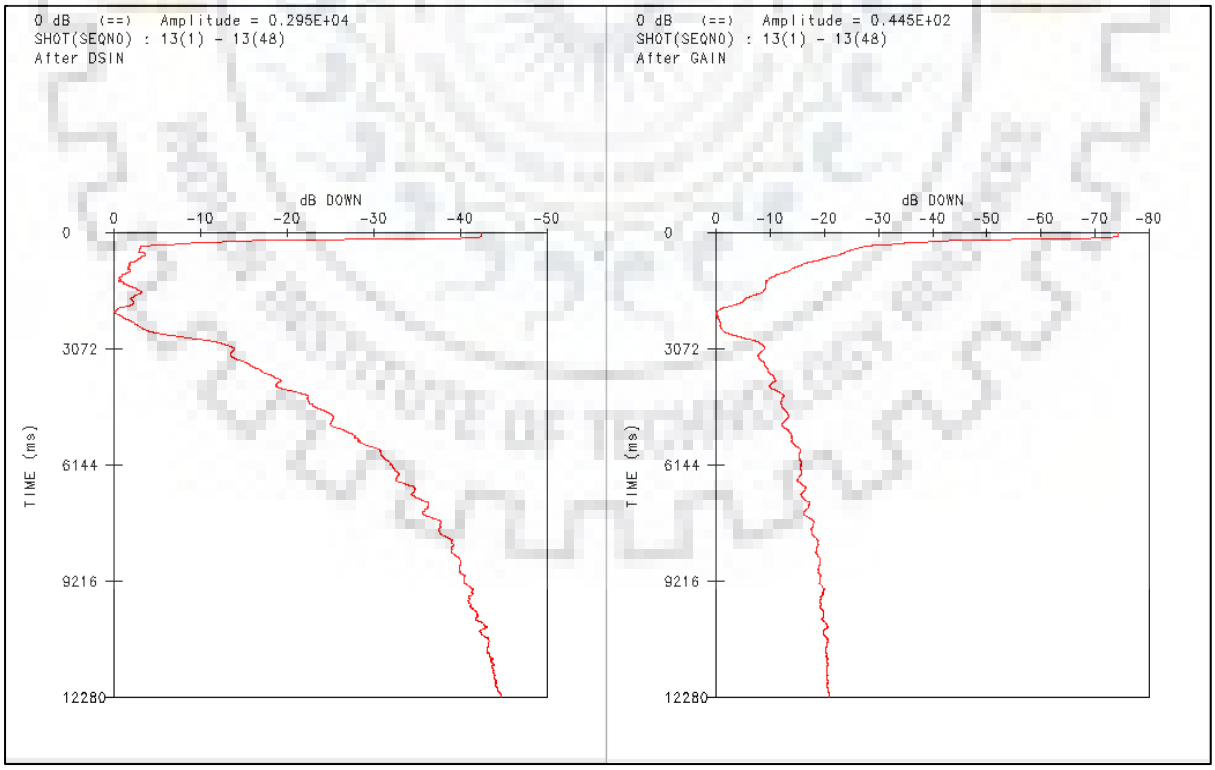


**Figure 3.1.11: Gain analysis before (left) and after (right) amplitude recovery.**

Where, $V_{rms}(T)$ = RMS velocity at time (T)

$V_o$ = RMS velocity at start-time (i.e. T = 0)

$VOPTION$ = Velocity power value (default is 2.0)

$TOPTION$ = Time power value (default is 1.0)

$$SCMAX = \frac{1}{SCALAR(T_{max})}$$

One must remember that “GAIN” boosts both signal and noise and further steps are needed to remove this noise (Fig.3.1.10). Gain analysis shows the changes in acoustic power of gathers before and after applying “GAIN” (Fig.3.1.11).

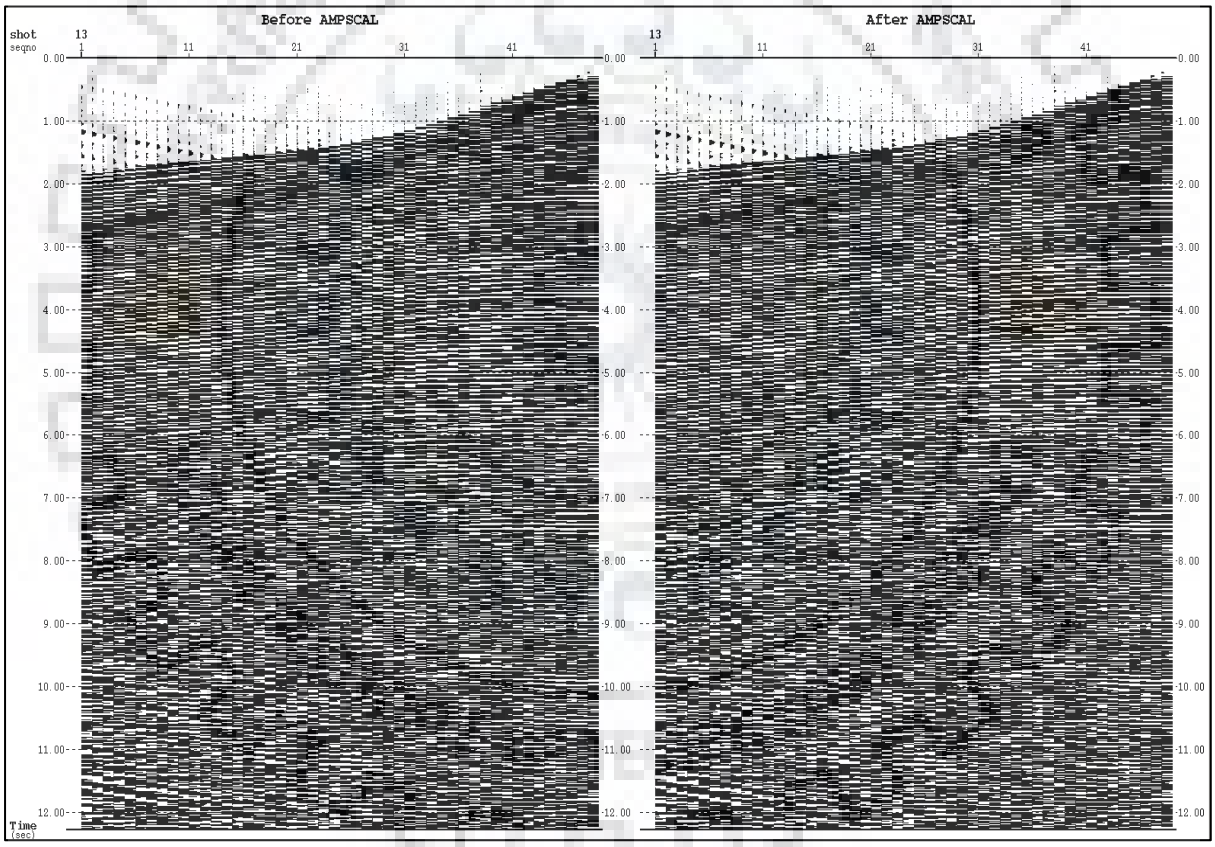


**Figure 3.1.12: Before (left) and after (right) amplitude scaling.**

There might be some noise bursts, cables slashes, air blasts, etc. which could spoil the quality of data. Such sporadic noises could be attenuated by using “AMPSCAL” module which scans for such abnormally high amplitudes and scales them down (Fig.3.1.12).

## 3.1.5. FILTERING & MUTE

A trapezoidal filter (as shown in Fig.3.1.13), is applied to remove any artefacts introduced. Filter frequencies were chosen by keeping in mind the aliasing filter (8-62 Hz) used for recording data. Using the “MUTE” module we pick and apply an “on-mute” to remove everything that is above the first break (Fig.3.1.14).

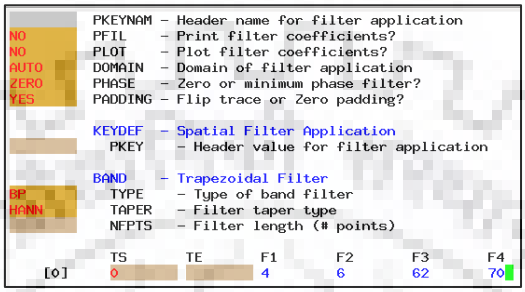


**Figure 3.1.13: Specifics of trapezoidal filter used for filtering (Source – Paradigm).**

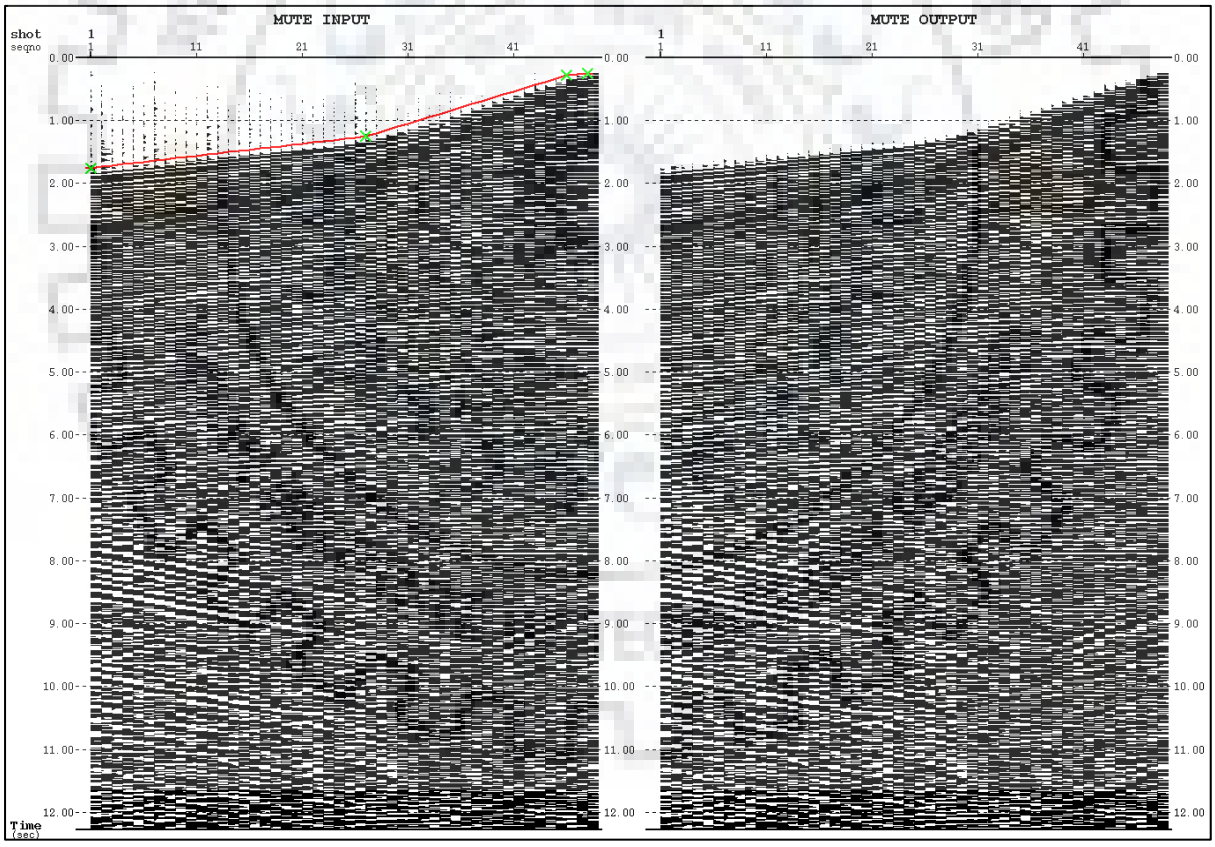


**Figure 3.1.14: Picking on-mute (left) and after applying mute (right).**

In latter sections, we would keep on using the same trapezoidal filter and mute for purpose of removing artefacts which might get introduced in data. In end, a brute stack is generated using near traces in order to get a rough idea about the

subsurface (Fig.3.1.15). For marine data, the source and receiver arrays are suspended at a constant depth throughout the survey and hence, static corrections are generally not required for marine data.

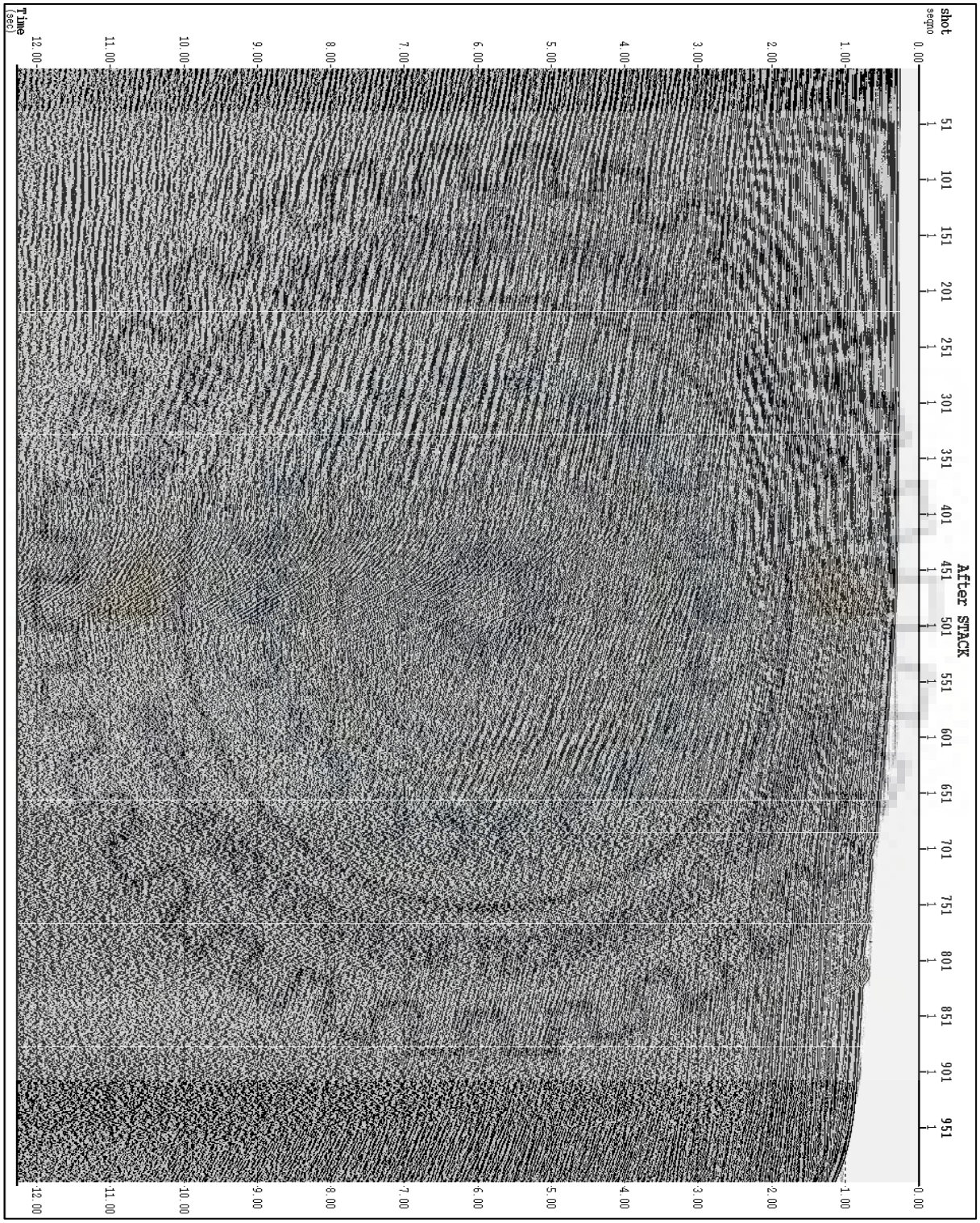


**Figure 3.1.15: Brute stack generated after pre-processing.**

# 3.2. PROCESSING

Pre-processing prepares data for future processing steps. Of all the processing steps the most important are deconvolution, stacking, and migration. The remaining processes could be considered secondary but they still help in conditioning of data and thus, increasing the quality of the aforementioned primary processes.

## 3.2.1. ATTENUATION OF LINEAR-COHERENT NOISE

Guided waves, direct-waves, head-waves, back-scattered waves are some examples of coherent linear noise that dominate marine datasets and hence, deserve special attention. Guided waves are basically a type of inference pattern formed by the waves trapped in the water layer (Fig.3.2.1).

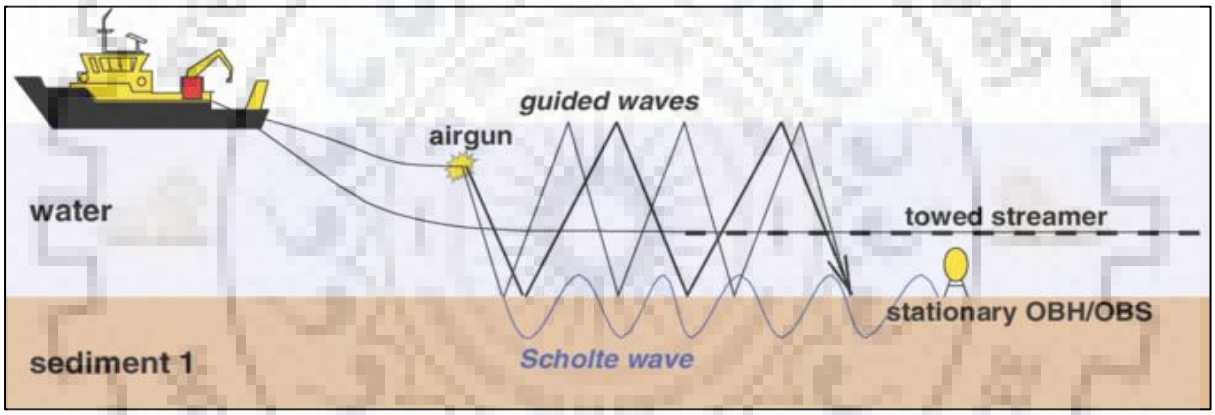


**Figure 3.2.1: Guided waves in shallow water acquisition (Source - http://bit.do/eSpGk).**

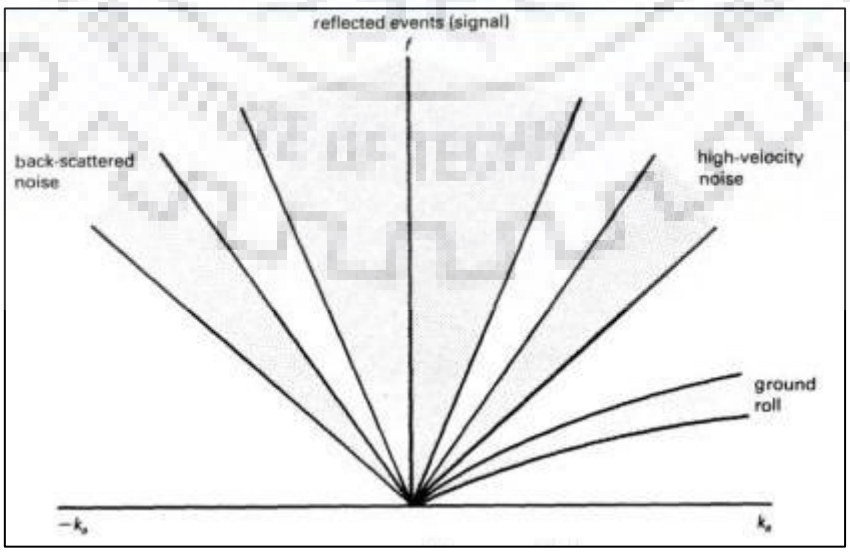


**Figure 3.2.2: Mapping of different seismic events in f – k domain (Reynolds, 1997).**

They are dispersive in nature and do not provide any useful information and their high amplitudes might end up masking the useful primary reflections. They can be removed by dip filtering in $f - k$ (frequency-wavenumber) domain (Fig.3.2.3) using the 'FKFILT' module. The result is largely free of reverberations and back-scatters (Fig.3.2.5).

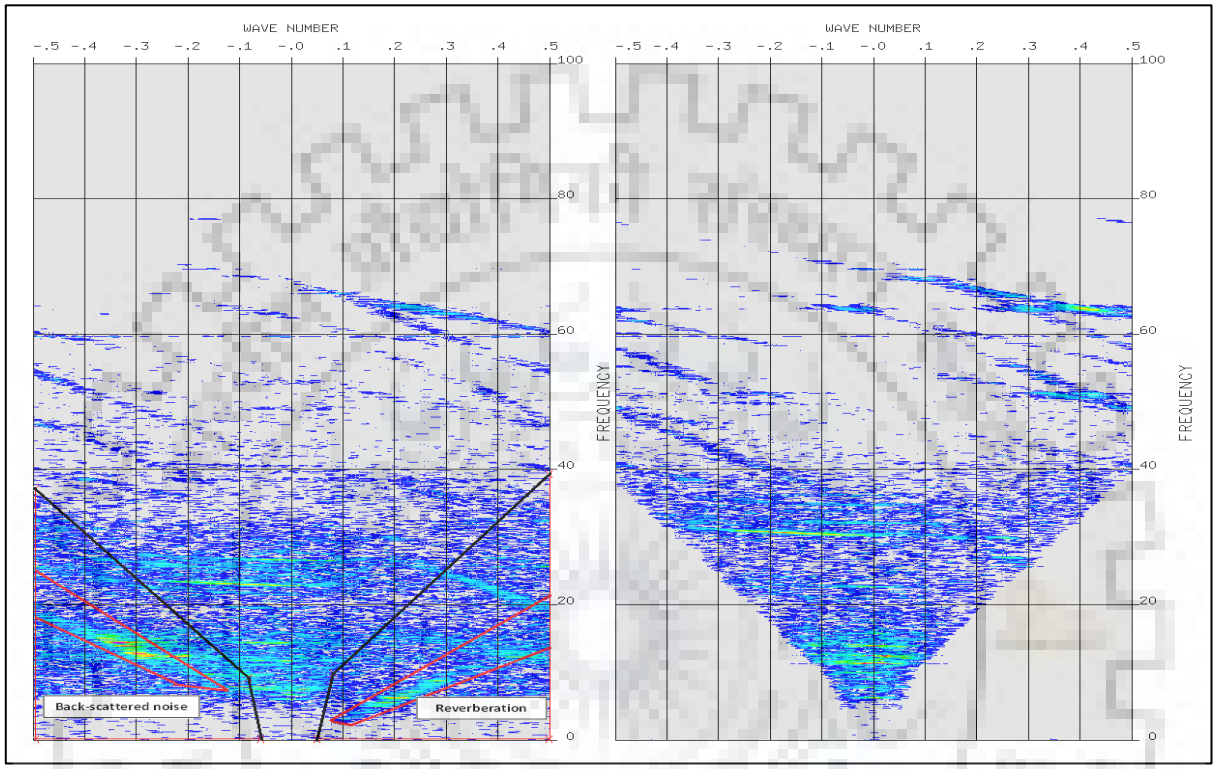


**Figure 3.2.3: Application of dip-filter (black in left image) in f – k domain.**

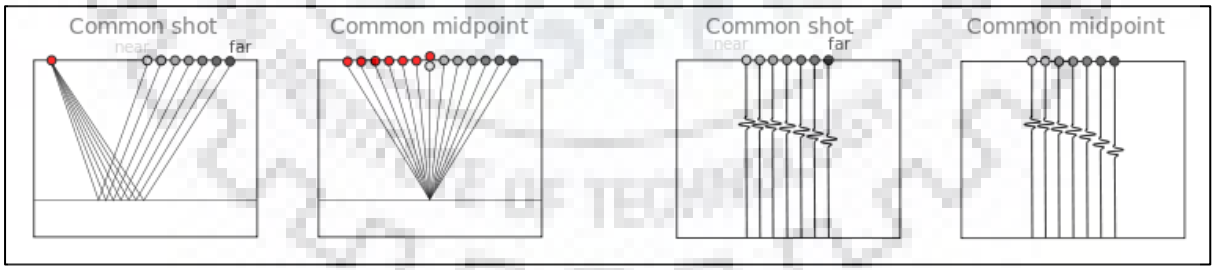


**Figure 3.2.4: Shot-gather and Common-midpoint (CMP) gather (Source- https://bit.ly/2E9AMu5).**

As can be seen in the image above, spatial aliasing is a major concern in dip filtering and hence, it is advised to apply such a filter on shot-gathers instead of CMP-gathers, given that the latter could have much larger trace-spacing compared to the former (Fig.3.2.4). A dip-filtered dataset yields better velocity analysis. But it is not enough and a good portion of linear noise still remains.

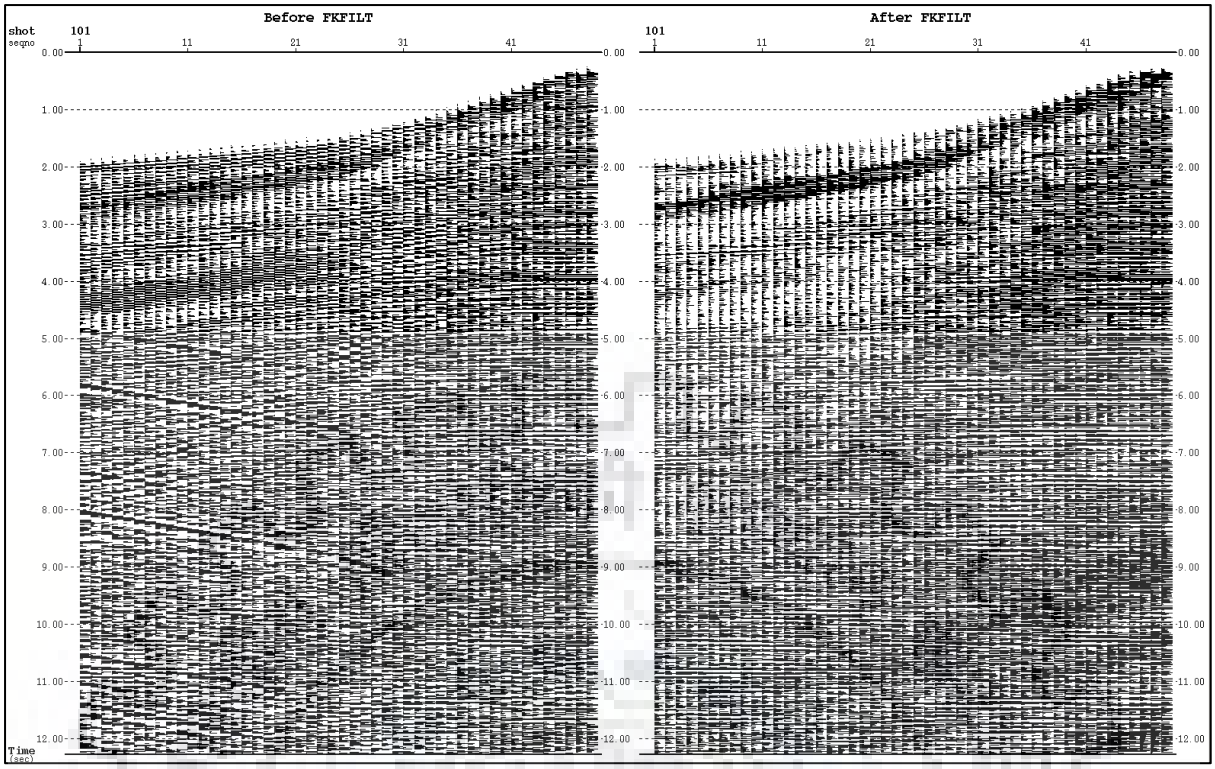


**Figure 3.2.5: Before (left) and after (right) f – k filtering.**

The $f - k$ transform maps data into $f - k$ i.e. frequency-wavenumber domain, whereas radon transform maps data into $\tau - p$ domain, where '$\tau$' is the intercept of two-way travel time & '$p$' is the ray-parameter. Such a transform can be performed in Paradigm using the "RADNLIN" module (step 2 in Fig.3.2.6). A linear event in a shot gather appears as a point in the $\tau - p$ domain, where it can be removed in a manner similar to dip-filtering using the "MUTE" module (step 3 in Fig.3.2.6). A vase shaped off-mute is picked (Fig.3.2.7) for rejecting the linear noise.

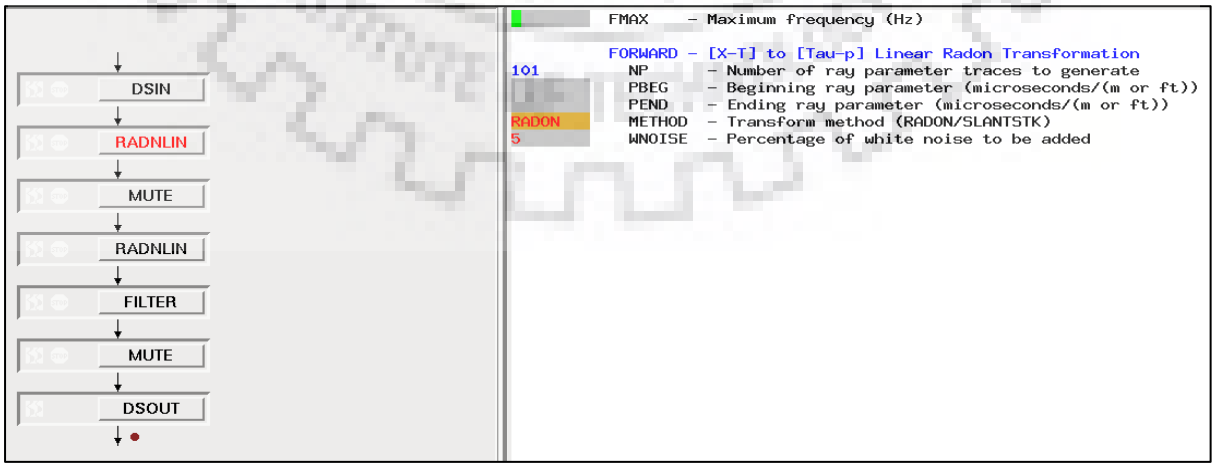


**Figure 3.2.6: Workflow of attenuating linear noise using radon transform, showing the value of parameters used for applying forward radon transform (Source - Paradigm).**

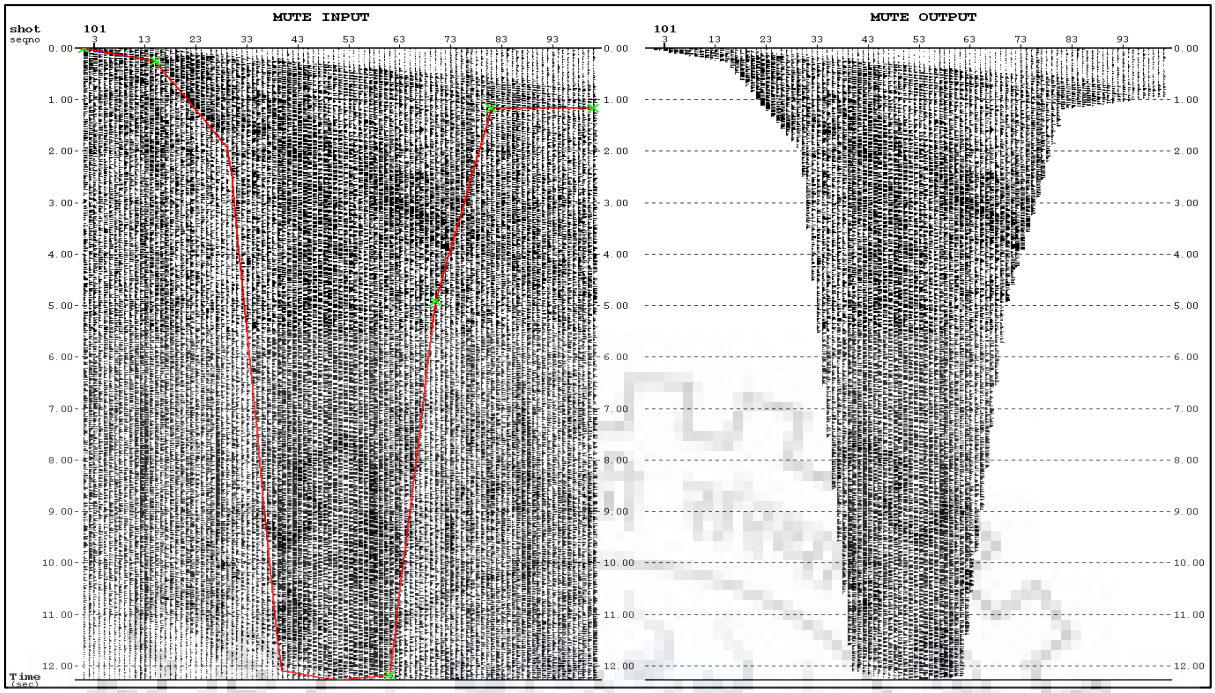


**Figure 3.2.7: Applying off-mute in τ – p domain to eliminate linear noise.**

Furthermore, when one map shot-gathers in a radon transform domain based on hyperbolic moveout, linear coherent noise and spatially random noise get excluded and as a result, a reconstructed gather (Fig.3.2.8) after inverse radon transform (step 4 in Fig.3.2.6) will be free of such noise.

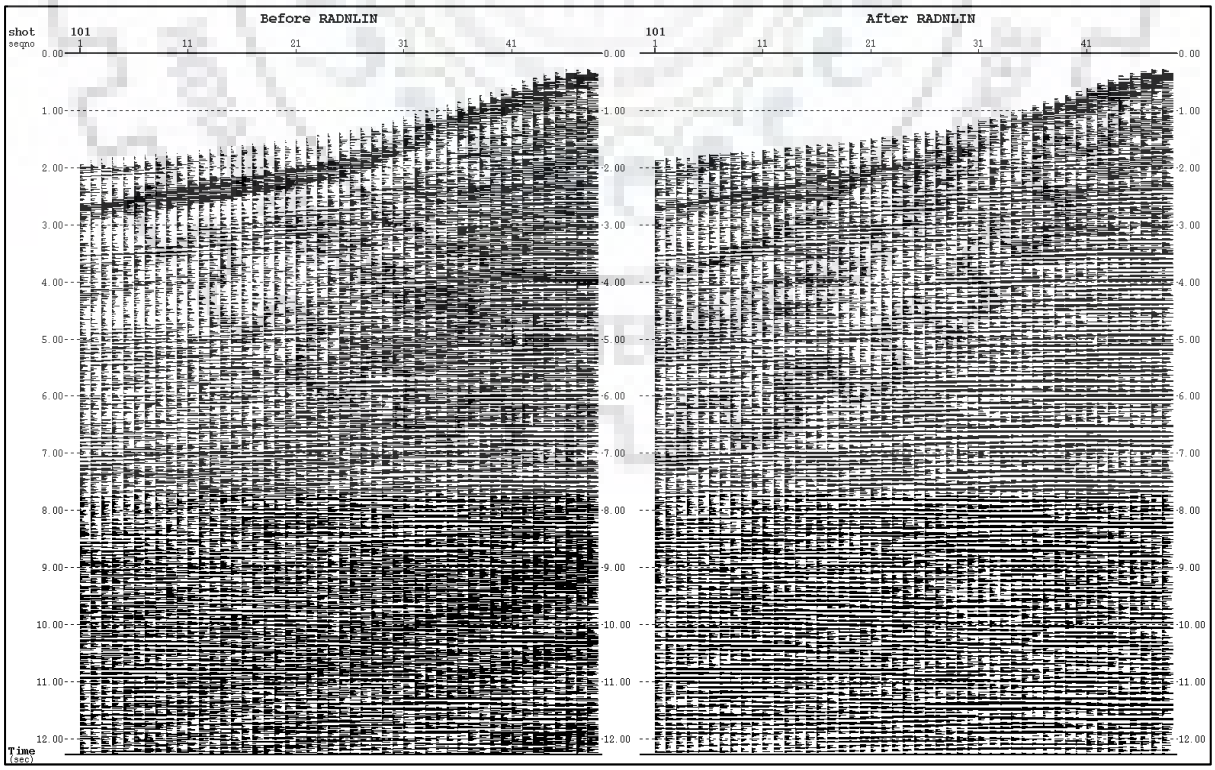


**Figure 3.2.8: Before (left) and after (right) removing linear noise using radon transform.**

## 3.2.2. DECONVOLUTION

Deconvolution is very important processing step. It compresses the basic source wavelet thus, increasing the bandwidth of the wavelet and as a result, also increases the temporal resolution of data. Such a deconvolution is called as “spiking” deconvolution. Mathematical formulation of deconvolution is shown below (Oz Yilmaz, 2001):

$$E(t) = k(t) * y(t) \tag{3.2.2.1}$$

Where, $k(t)$ is a filter operator defined such that convolution of $k(t)$ with the known seismogram $y(t)$ yields an estimate of the earth’s impulse response $E(t)$.

$$y(t) = w(t) * E(t) \tag{3.2.2.2}$$

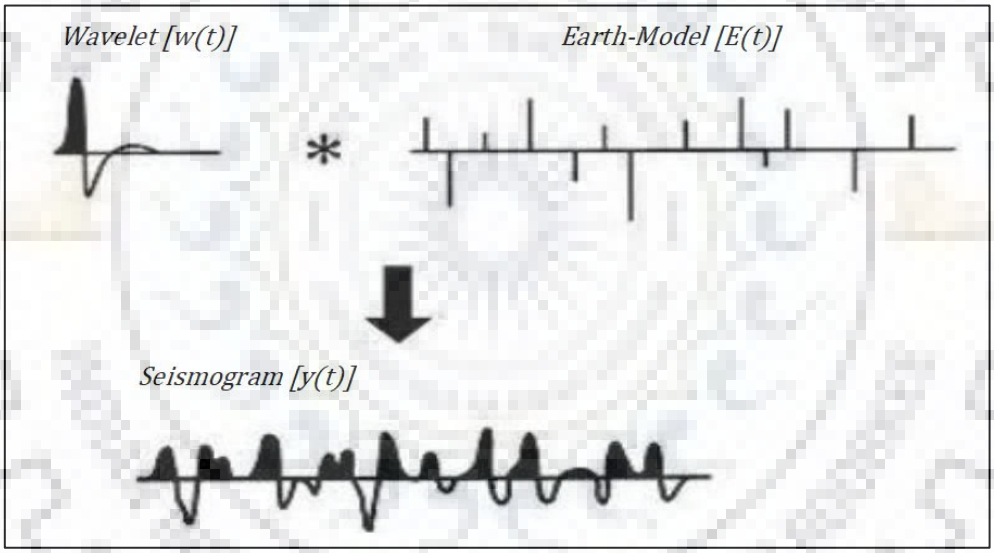


**Figure 3.2.9: A diagram of equation (3.2.2.2) showing the recorded seismogram y(t) as a product of convolution of source wavelet w(t) and earth’s model i.e. reflectivity E(t) (Yilmaz, 2001).**

Where, $y(t)$ the input seismogram is a result of convolution of input seismic wavelet $w(t)$, and the earth’s impulse response $E(t)$ (Fig.3.2.9). By substituting equation (3.2.2.1) into equation (3.2.2.2), we will get:

$$y(t) = w(t) * k(t) * y(t) \tag{3.2.2.3}$$

When $y(t)$ is eliminated from both sides of the equation, the following expression results:

$$\delta(t) = w(t) * k(t) \qquad (3.2.2.4)$$

Where, $\delta(t)$ represents the Kroneckel delta function. By solving equation (3.2.2.4) for the filter operator $k(t)$ we obtain:

$$k(t) = \delta(t) * (1/w(t)) \qquad (3.2.2.5)$$

Thus, it can be said that the filter operator $k(t)$ is the mathematical inverse of the input seismic wavelet $w(t)$. If the input seismic wavelet is known as in case of vibroseis source, then it is called as deterministic deconvolution, but if it is estimated statistically from the input seismogram then it is called as statistical deconvolution. From equation (3.2.5) we can say that deconvolution is an inverse filter.

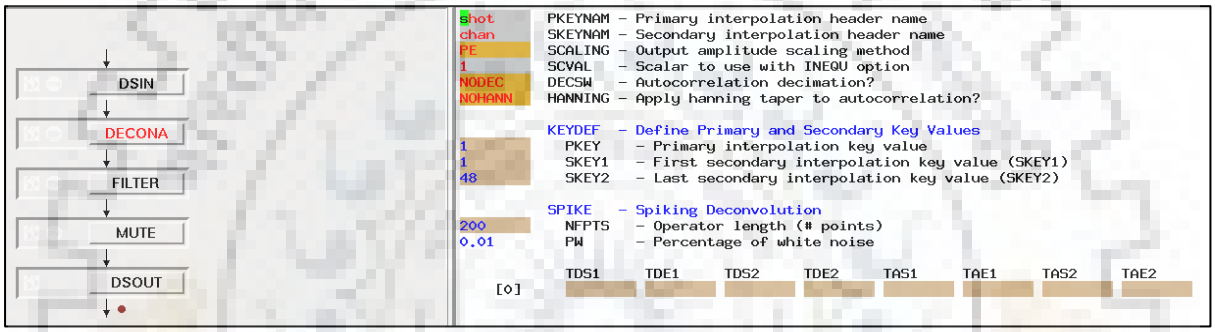


**Figure 3.2.10: Workflow of applying spiking deconvolution (Source – Paradigm).**

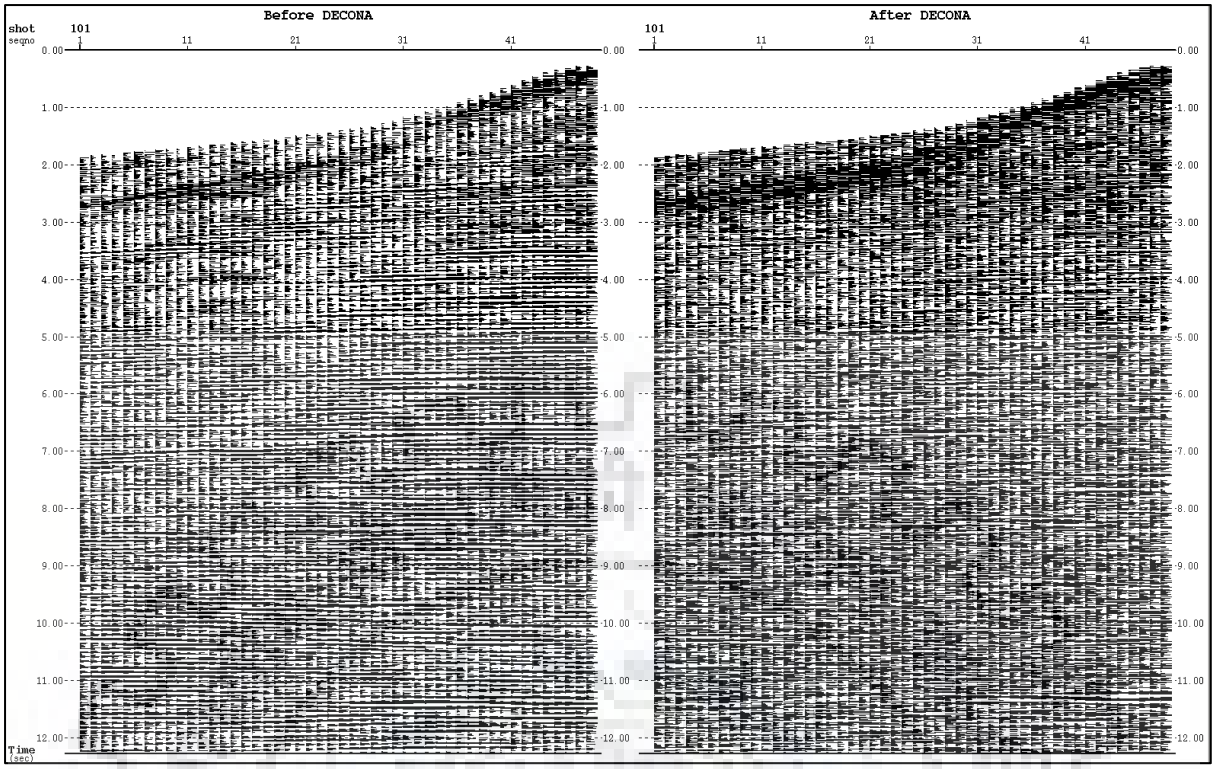


**Figure 3.2.11: Before (left) and after (right) applying spiking deconvolution.**

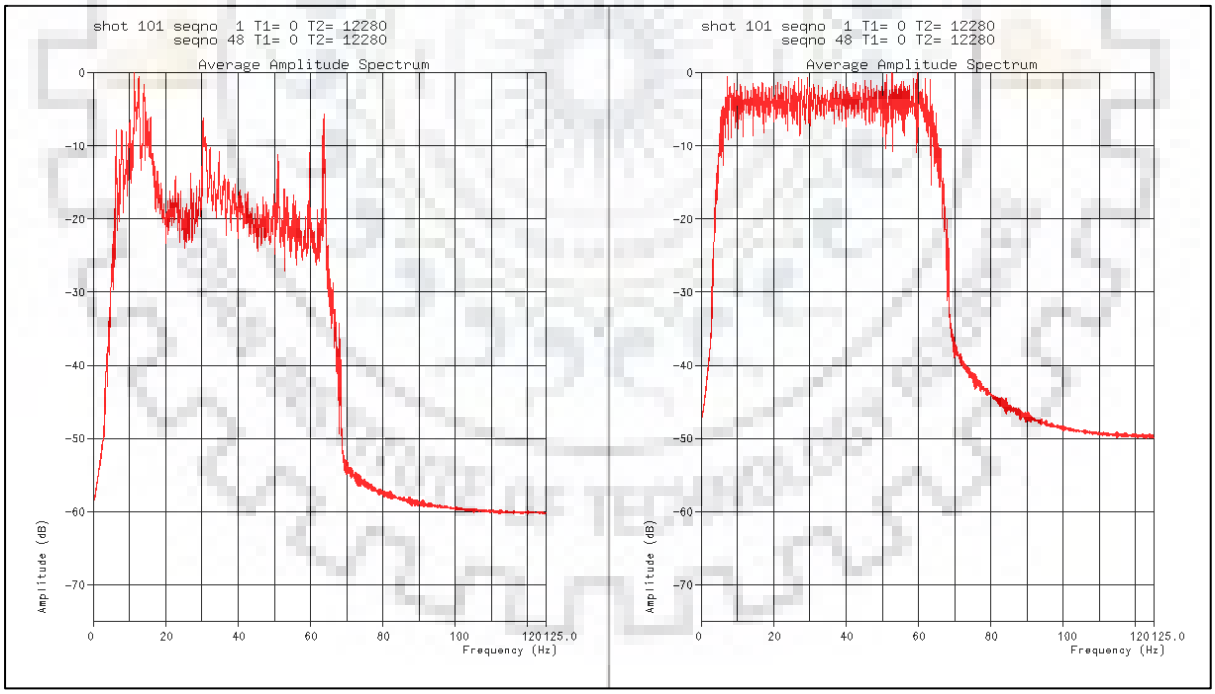


**Figure 3.2.12: Amplitude spectra before (left) and after (right) applying spiking deconvolution.**

In Paradigm deconvolution is applied using the "DECONA" module (Fig.3.2.10), which allows us to design filters and applies them in a trace by trace manner. After the spiking deconvolution, primary events become sharper while at the same time,

the trailing reverberations are attenuated (Fig.3.2.11). Spiking deconvolution flattens the amplitude spectra of the gather (Fig.3.2.12). Hence, it is also known as “whitening” deconvolution.

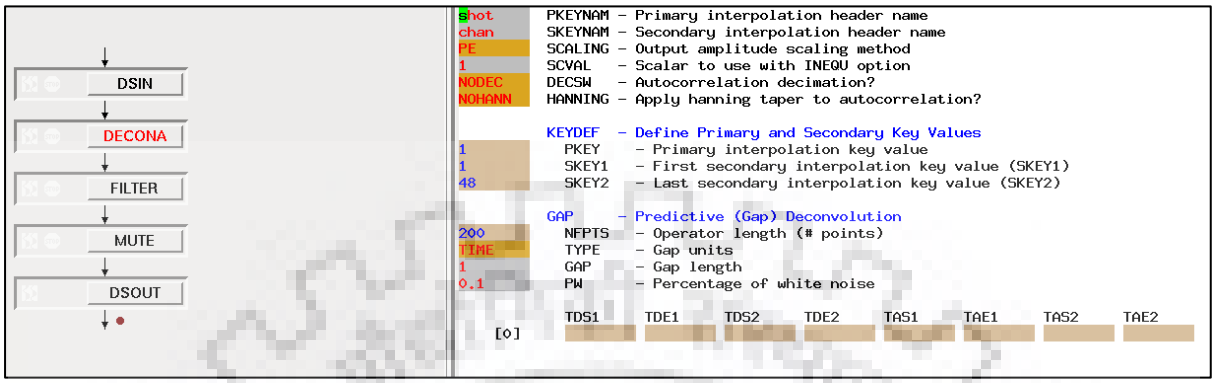


**Figure 3.2.13: Workflow of applying gapping deconvolution (Source - Paradigm).**

A deconvolution operator with a predictive lag is called “gapping” deconvolution. The “DECONA” module allows for creating a gapping filter (Fig.3.2.13). It can significantly attenuate ghosts, instrument effects, reverberations and multiples (Fig.3.2.14) by exploiting their periodic nature and creating a predictive filter. Hence, it is also known as “predictive” deconvolution. Like spiking deconvolution, it too flattens the amplitude spectra of data (Fig.3.2.15).

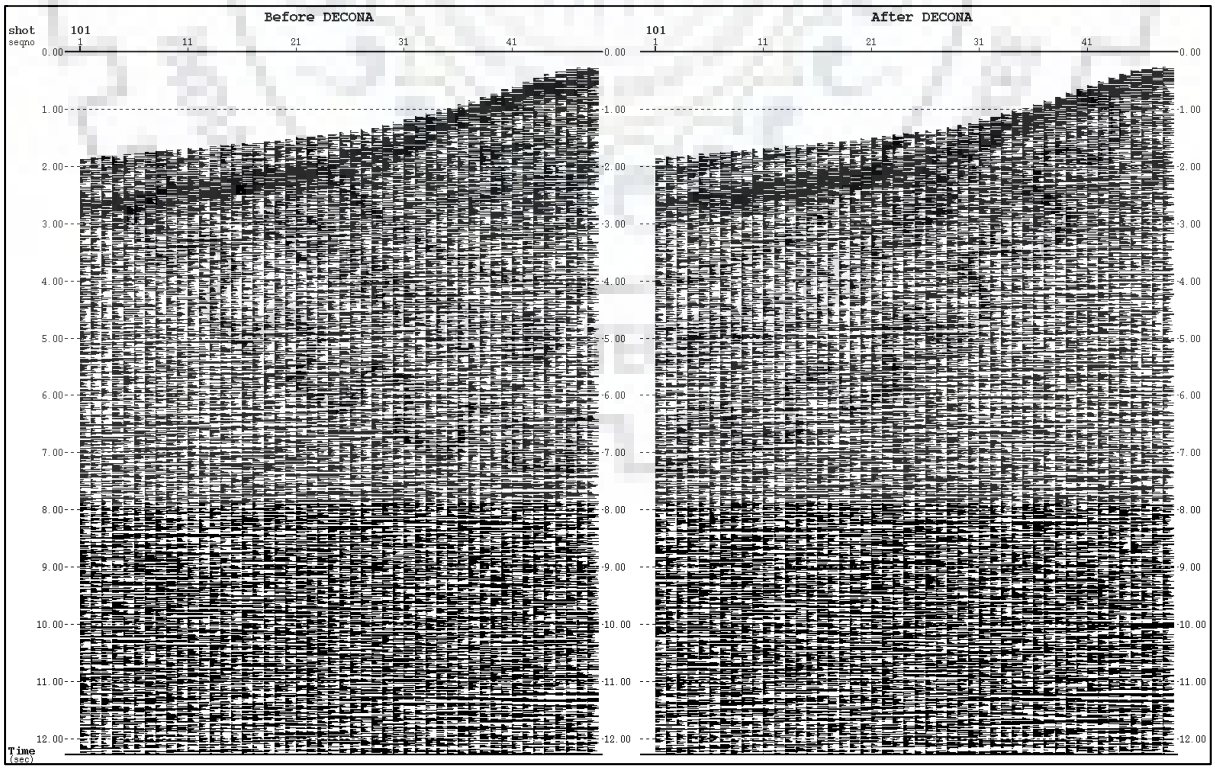


**Figure 3.2.14: Before (left) and after (right) applying gapping deconvolution.**

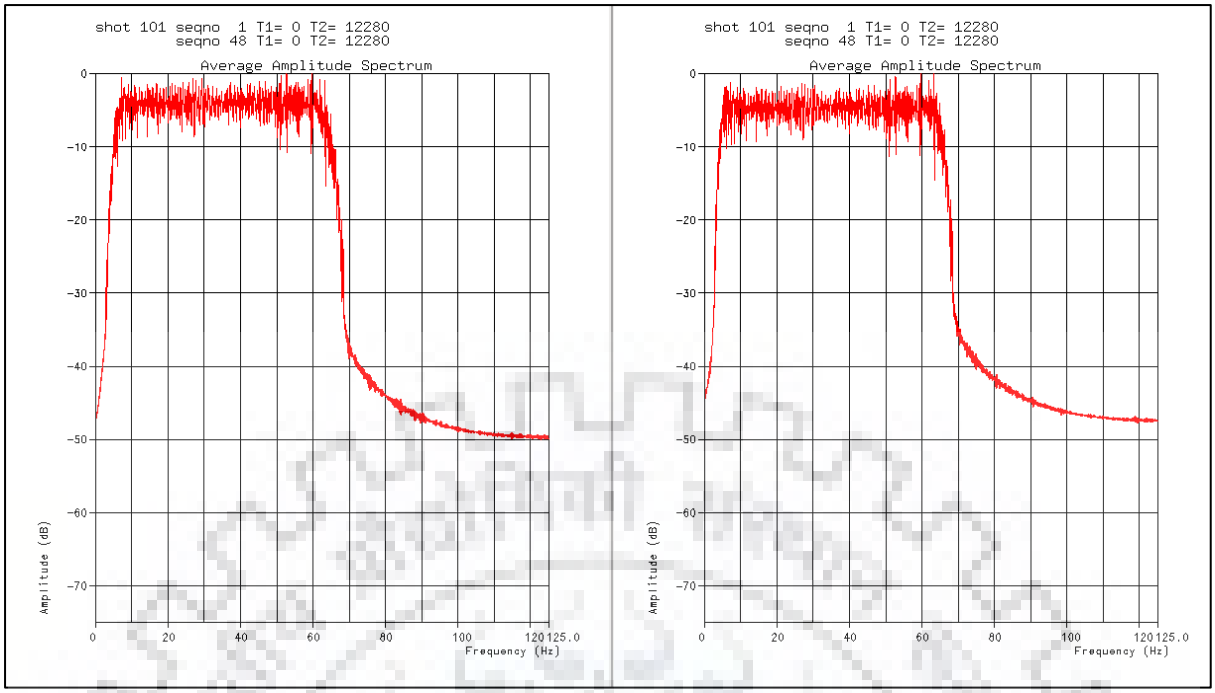


**Figure 3.2.15: Amplitude spectra before (left) and after (right) applying gapping deconvolution.**

Despite the benefits that it provides, deconvolution also boosts the low and high frequency noise; and even after applying the previously mentioned (see "3.1.5. Filtering and Mute") trapezoidal filter and mute (step 2 and 3 in Fig.3.2.10 & Fig.3.2.13) some artefacts may still remain. Keeping this trade-off in mind, it is advisable to not to make frequent use of deconvolution within a given dataset.

## 3.2.3. DE-GHOSTING

Under the ocean surface, the acoustic waves are travelling in a medium with a velocity of about 1500 m/sec and a density close to 1 g/cc, whereas above it in the air, the velocity is about 340 m/sec and density is approxiamtely 0.0013 g/cc. By substituting these values in the reflection coefficient (RC) equation (3.2.3.1), we find that reflection coefficient for free surface is about 0.9994, which makes it almost a perfect reflector.

$$RC = \frac{\rho_2 v_2 - \rho_1 v_1}{\rho_2 v_2 + \rho_1 v_1} \qquad (3.2.3.1)$$

Where, $\rho_i$ and $v_i$ are density and velocity of $i^{th}$ layer, respectively.

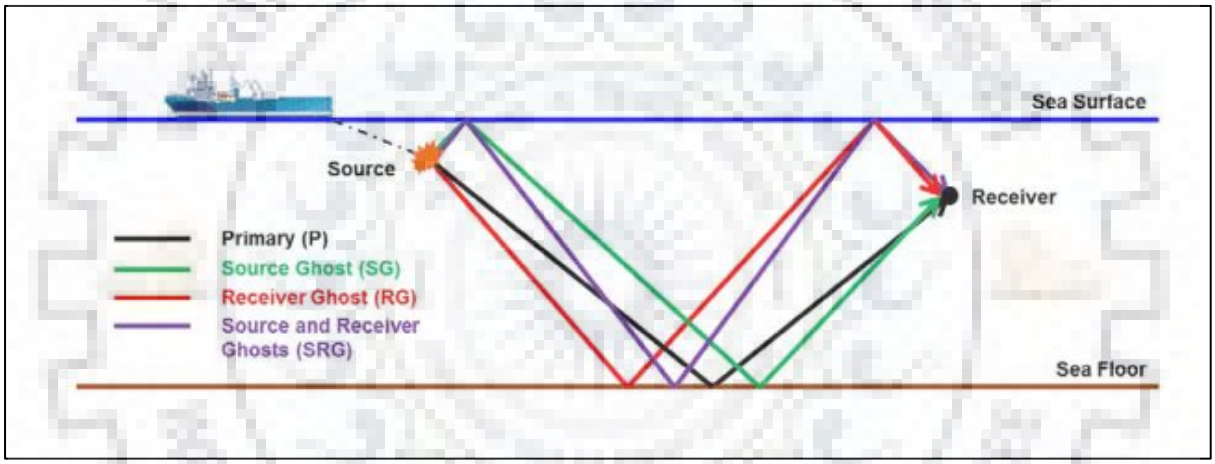


**Figure 3.2.16: Ray paths of source and receiver ghosts (Source - http://bit.do/eSpJe).**

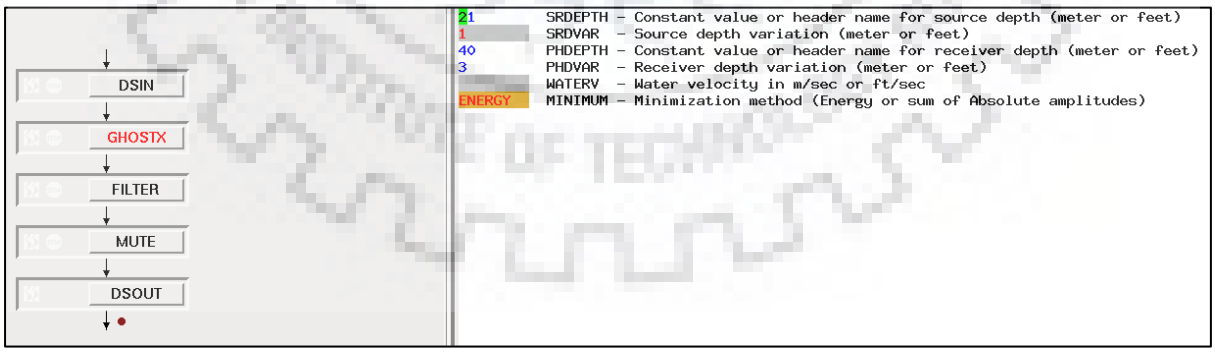


**Figure 3.2.17: Workflow of de-ghosting using "GHOSTX" module (Source - Paradigm).**

Ghosts are a series of spurious reflections of seismic energy that are reflected back from this free surface. Starting from the source, when the upward traveling waves reflect from the ocean surface, they follow the originally downgoing waves, but with a

certain delay and hence, appear as a double image. These are known as source ghosts (Fig.3.2.16). Similarly, the waves that arrive at receiver locations, continue moving upward and are recorded again after reflecting from ocean surface. These are known as the receiver ghosts (Fig.3.2.16).

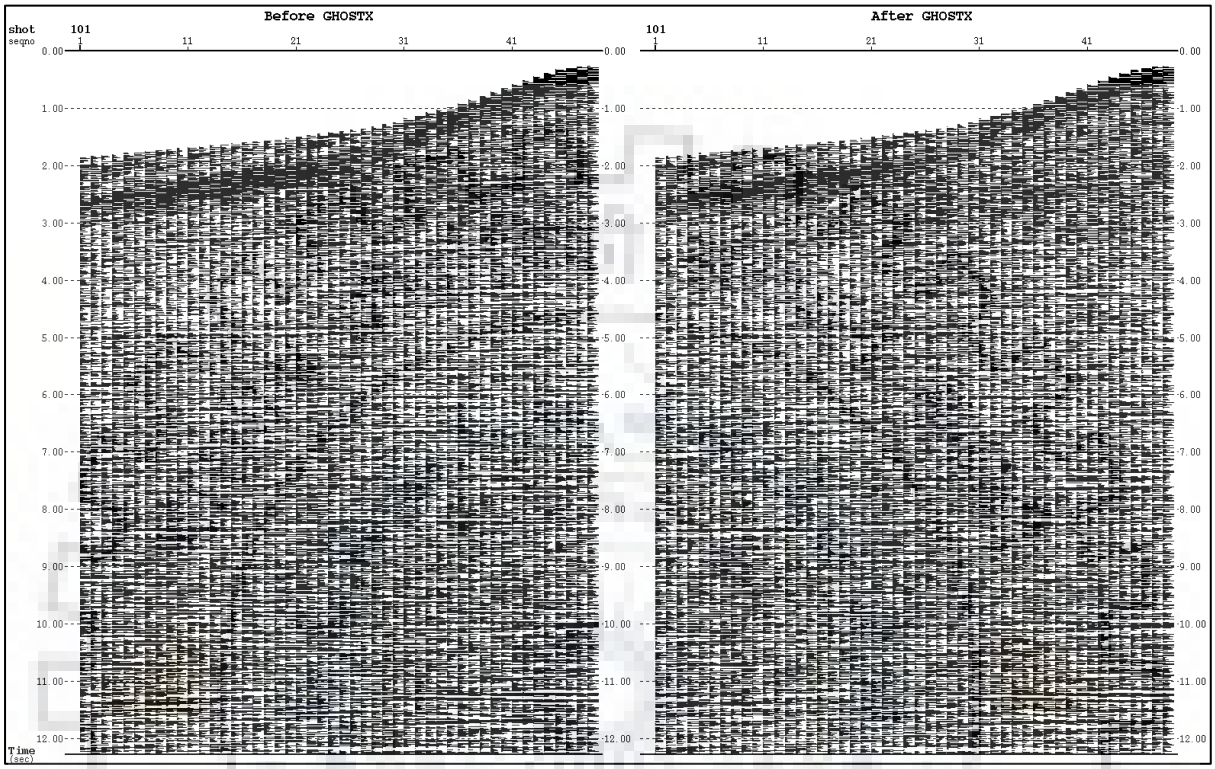


**Figure 3.2.18: Before (left) and after (right) de-ghosting.**

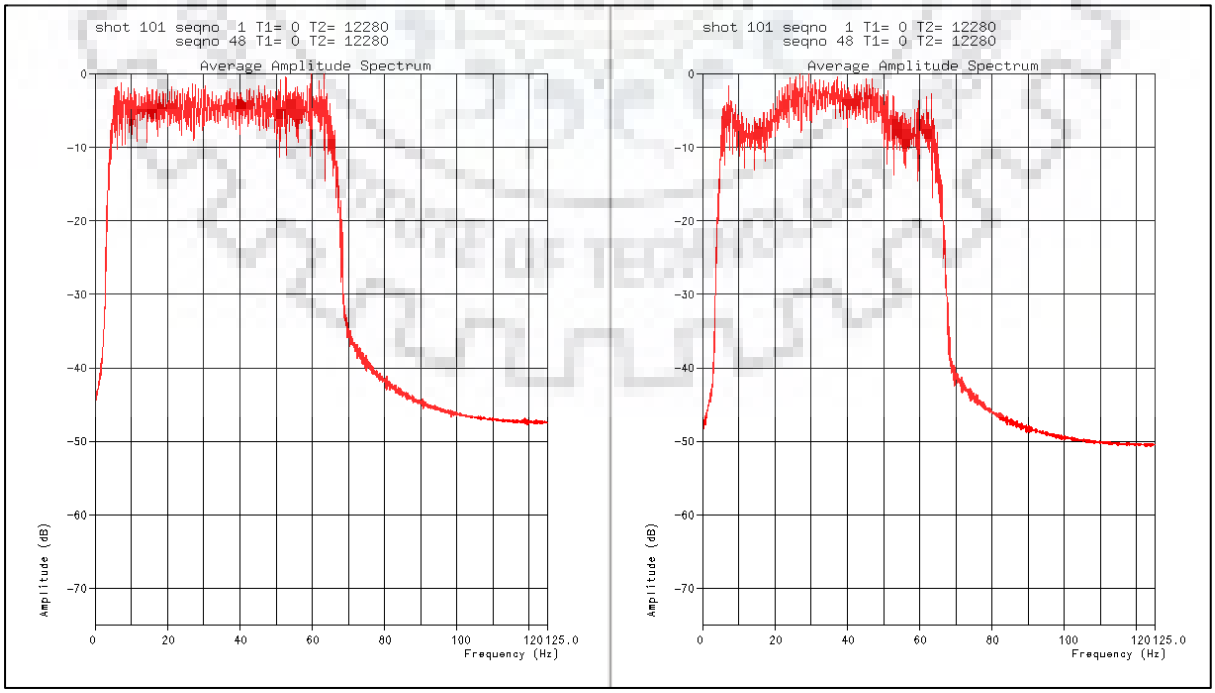


**Figure 3.2.19: Amplitude spectra before (left) and after (right) de-ghosting.**

Ghost reflections interfere with primaries and must be removed. In Paradigm, de-ghosting is performed using the “GHOSTX” module (Fig.3.2.17). It uses least square minimization to determine source & receiver ghost times as well as reflection coefficient at free surface for both of these ghost waves. It is employed mostly on shot gathers after eliminating linear noise. The result of ghost elimination and its spectral analysis are shown in figures 3.2.18 and 3.2.19, respectively.

## 3.2.4. VELOCITY ANALYSIS

All of the processes above were performed in shot domain i.e. on shot-gathers, but starting from velocity analysis we would work in CMP domain i.e. on CMP-gathers. Therefore, we first sort the shot-gathers into CMP-gathers (Fig.3.2.20).

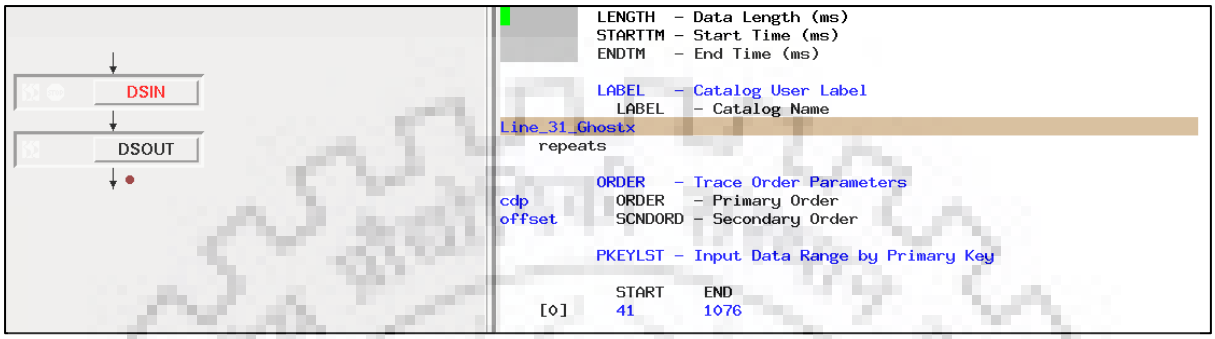


**Figure 3.2.20: Sorting shot-gathers into CMP-gathers (Source - Paradigm).**

For successful depth estimation we need to know the velocity of seismic waves and its variation with depth. The theory of velocity analysis is based on the hyperbolic moveout of a nearly horizontal event on a CMP-gather, given by equation (3.2.4.1):

$$T_x{}^2 = \frac{X^2}{(V_{NMO})^2} + T_o{}^2 \qquad (3.2.4.1)$$

Where, $T_x$ = Travel time (for offset = $X$) $T_o$ = Travel time for zero-offset

$X$ = Source-receiver offset $V_{NMO}$ = Stacking/NMO velocity

$$\Delta T_{NMO} = T_x - T_o \qquad (3.2.4.2)$$

By using Taylor approximation of equation (3.2.4.1) and substituting the value of $T_x$ in equation (3.2.4.2), we get:

$$\Delta T_{NMO} \approx \frac{X}{2T_o V_{NMO}} \qquad (3.2.4.3)$$

Where, $\Delta T_{NMO}$ = Normal-moveout (NMO) correction (Fig.3.2.21).

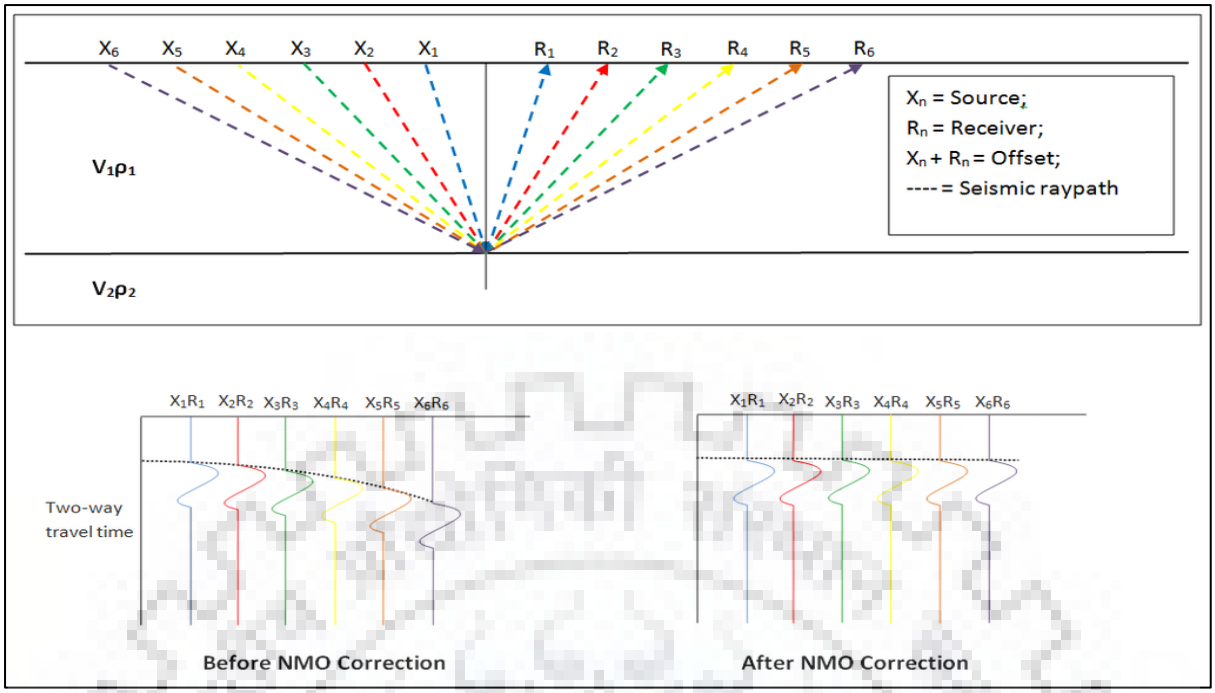


**Figure 3.2.21: Applying normal-moveout (NMO) correction on CMP gather (Source – SEG wiki).**

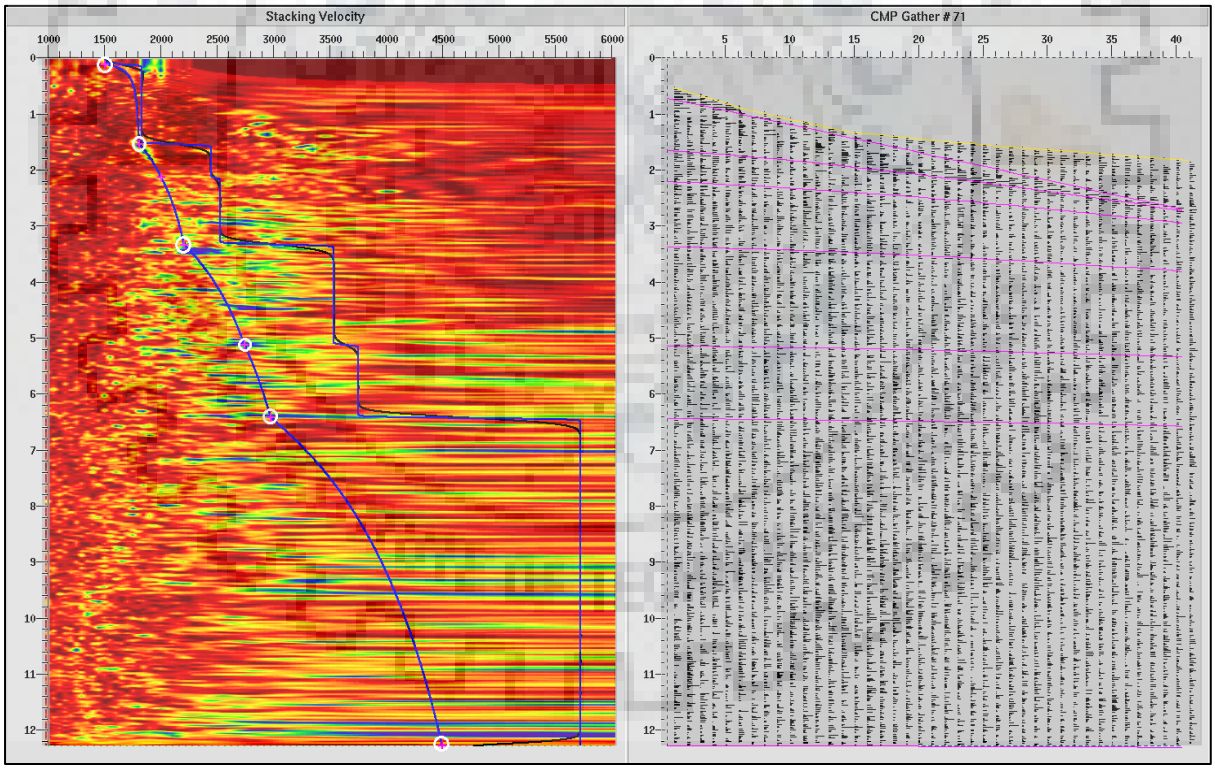


**Figure 3.2.22: Picking stacking velocities (white circles) using semblance (left) and the corresponding moveouts (pink lines) displayed on CMP-gather (right).**

We start by picking stacking velocity (Fig.3.2.22), and subtracting the estimated value of NMO correction; from equation (3.2.4.3); from total travel-time. The value of stacking velocity is chosen such that the corresponding primary event should flatten

(Fig.3.2.23) after applying NMO correction. Since, this correction is a function of reflector depth, stacking velocity and source-receiver offset, it has to be calculated for every time sample of a seismic trace. Thus, picking accurate velocities at various depths is a necessity. Few points to keep in mind while picking velocity using semblance plot:

- Pick velocities where semblance is high.
- Pick velocities such that after applying NMO the reflector appears horizontal.
- Semblance contamination due to multiples, réverbérations etc.

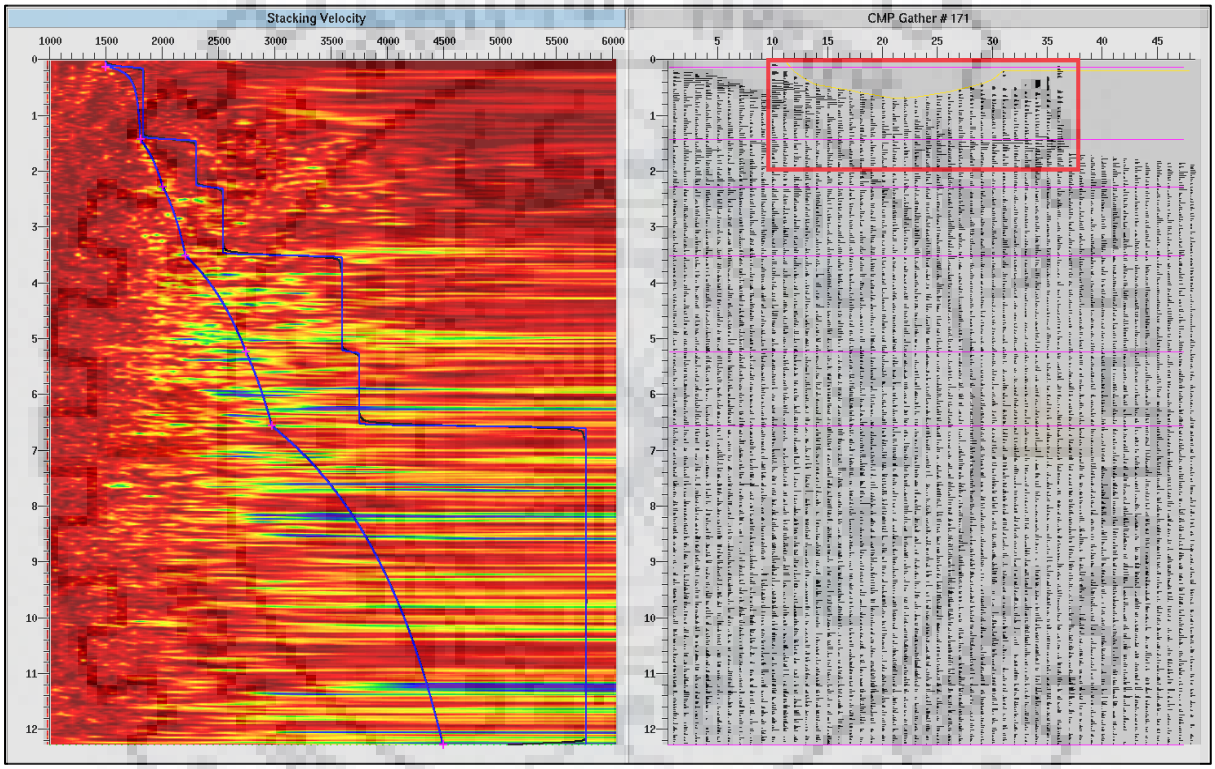


**Figure 3.2.23: After applying NMO correction (right) using preciously mentioned stacking velocities. The image also displays NMO-stretching (red box) in far-traces at shallow depths.**

Paradigm also allows for estimating root-mean-square velocity $(V_{RMS})$ from the previously picked stacking velocity. RMS velocity is a mathematical model that takes into account Snell's law of refraction. It is defined by Dix (1955) as:

$$(V_{RMS})^2 = \frac{1}{T}\int_{t=0}^{t=T}(V_{ins}(t))^2 . dt \qquad (3.2.4.4)$$

Where, $V_{ins}$ = Instantaneous velocity (as a function of time (t))

$T$ = Total travel-time.

The NMO correction causes frequency distortion, particularly for shallow reflectors with large offsets (Fig.3.2.23 & Fig.3.2.24). This phenomenon is known as NMO-stretching. The amount of stretch is indicated by increase in the number of samples compared to original number of samples. As a result of this stretching, stacking of NMO corrected CMP gathers, will severely distort the shallow events. This problem can be overcome by applying a NMO-stretch mute (Fig.3.2.24) to reject the stretched zone in gather. Paradigm provides option for automatically removing stretch just by specifying the permissible stretch limit or one may choose to do this manually, as we have done here (Fig.3.2.24). After removing the NMO-stretch, the data is ready to stack.

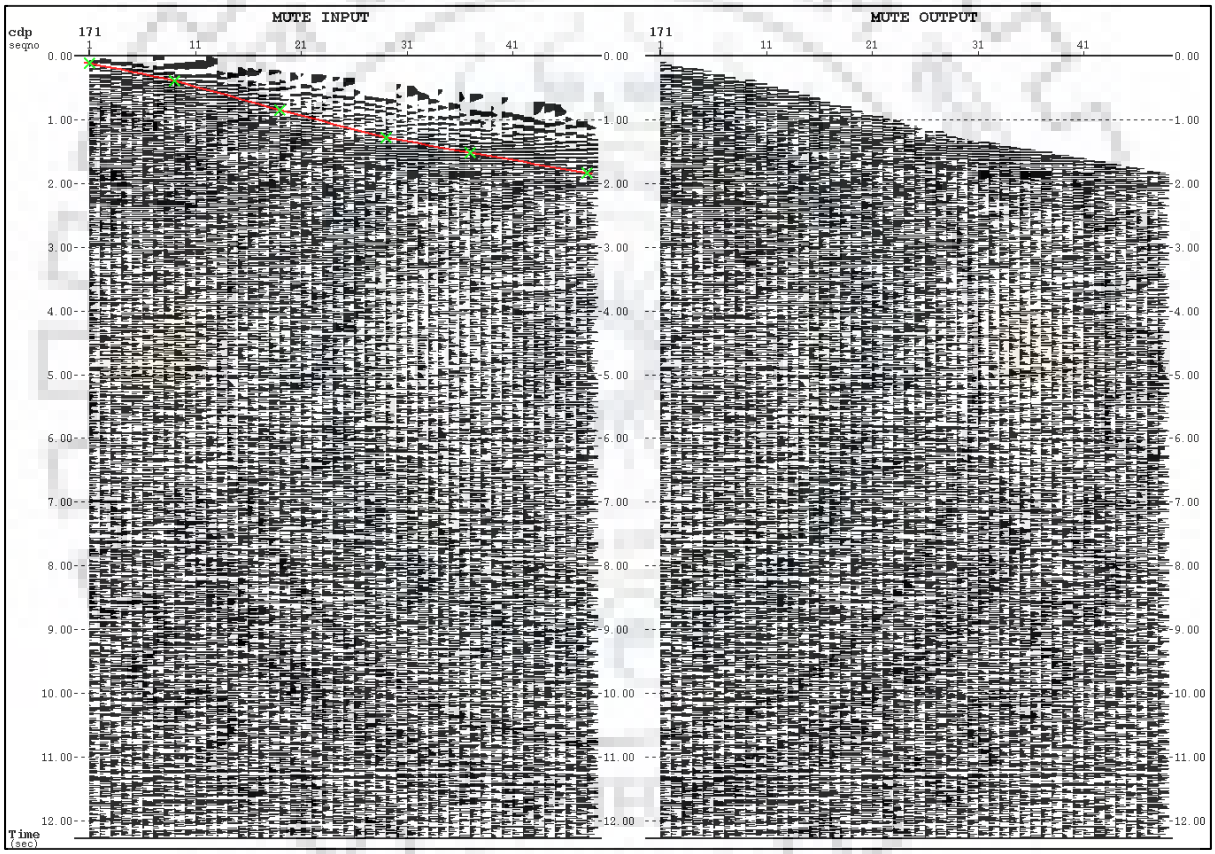


**Figure 3.2.24: Before (left) and after (right) applying NMO-stretch mute.**

## 3.2.5. STACKING

Stacking is a process of compressing CMP-gathers by summing all traces it contains, which have already been corrected for their respective normal moveouts, to a zero-offset trace. Stacking enhances the in-phase components and reduces the random noise. Coherent noise like multiples and guided waves have larger moveouts and hence, they are not flattened after NMO correction. As a result, they also get attenuated after stacking. This makes stacking is the most effective method of improving signal-to-noise ratio of multichannel seismic data.

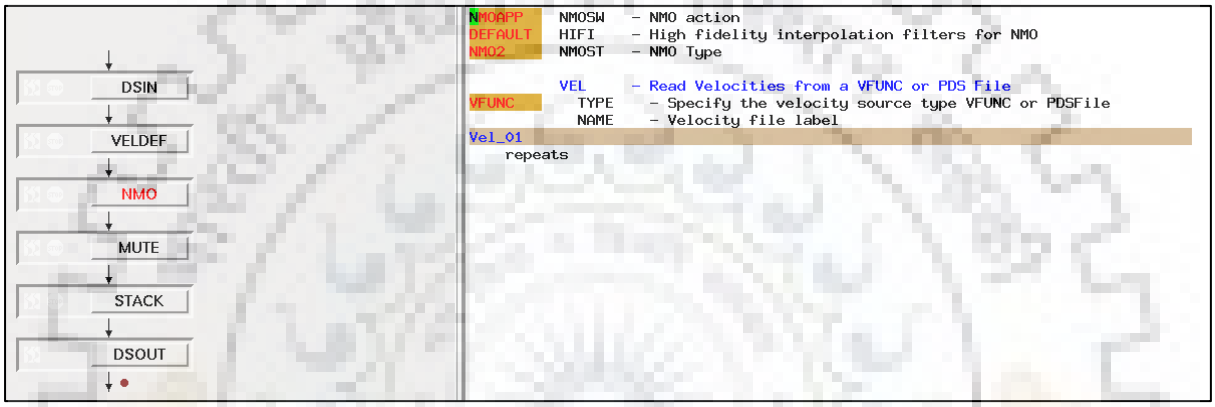


**Figure 3.2.25: Workflow of stacking using "STACK" module. The diagram also shows the velocity function used for applying NMO correction before stacking (Source - Paradigm).**

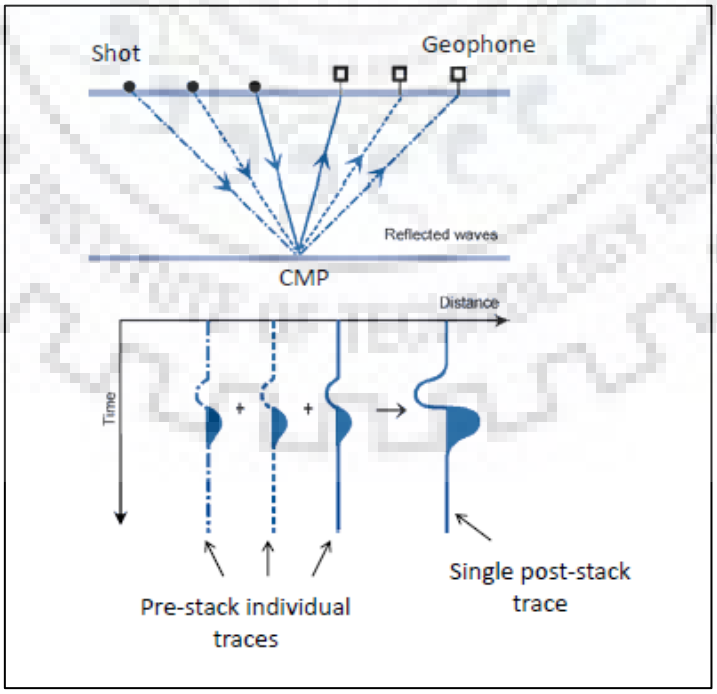


**Figure 3.2.26: Summing individual traces of CMP-gather to generate a single stacked trace (Source - http://bit.do/eSpMS).**

The “STACK” module is used (Fig.3.2.25) to create stack section. It algebraically sums the traces and outputs a single trace for each input ensemble i.e. CMP-gathers (Fig.3.2.26). Greater the foldage, greater is the increase in signal to noise ratio.

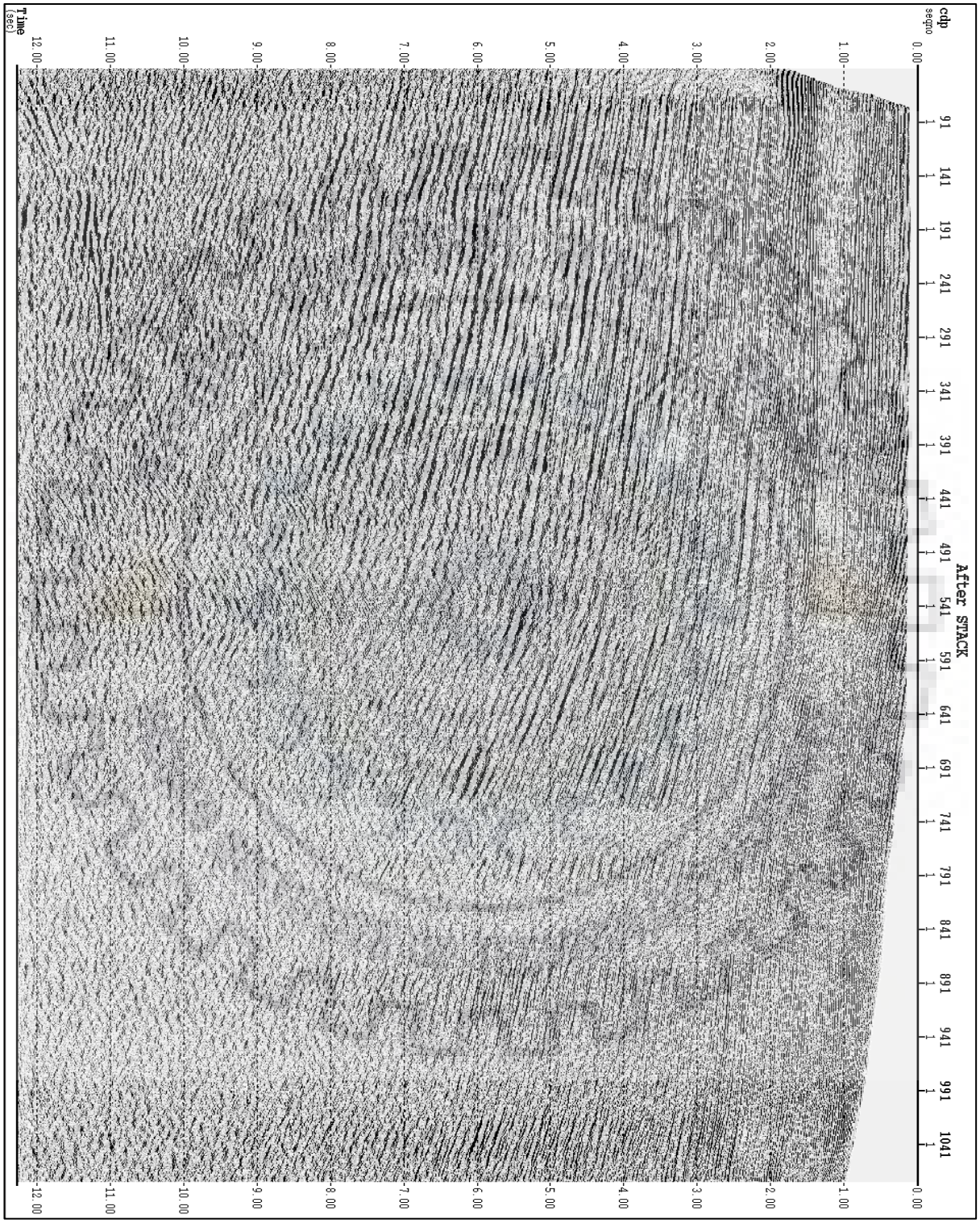


**Figure 3.2.27: Stacked image showing seismic cross-section of line 31.**

Figures (3.2.27) & (3.2.28) show the stacked seismic image of line 31; and in addition to this, the latter also shows the velocity profile of the section. This velocity profile is generated using the previously picked stacking velocities (discussed in "3.2.4. Velocity Analysis").


**Figure 3.2.28: Stacked image of line 31 along with its velocity profile.**

## 3.2.6. MIGRATION

The aim of seismic migration is to create a more accurate image of subsurface by moving the dipping reflectors to their supposedly true locations; i.e. where the said event must have taken place in the subsurface; from their apparent locations as perceived from the surface record. The need for such a correction arises because of a basic assumption involved in processing which assumes that subsurface reflectors are horizontal or nearly horizontal with minimal dip. Then going by this assumption, it follows that the reflections must come from the source-receiver midpoint (Fig.3.2.29 (a)). However, this assumption breaks down in case of a region where horizons have considerable dips (Fig.3.2.29 (b)).

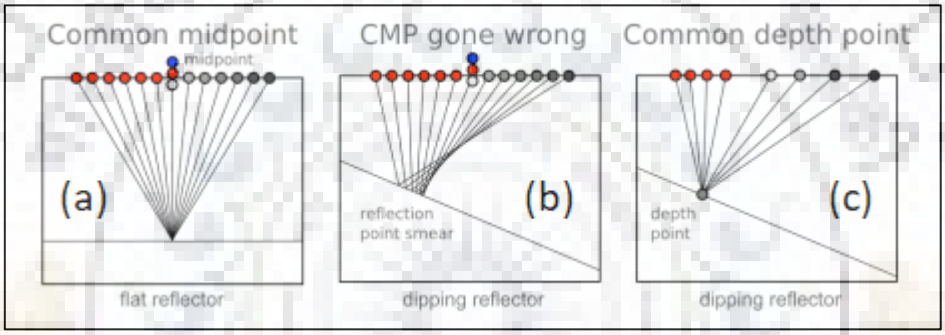


**Figure 3.2.29: (a) Common midpoint gather for a horizontal reflector; (b) Common midpoint gather for a dipping reflector; (c) Common depth-point gather consisting of source-receiver pairs with common reflection point (Source - https://bit.ly/2E9AMu5).**

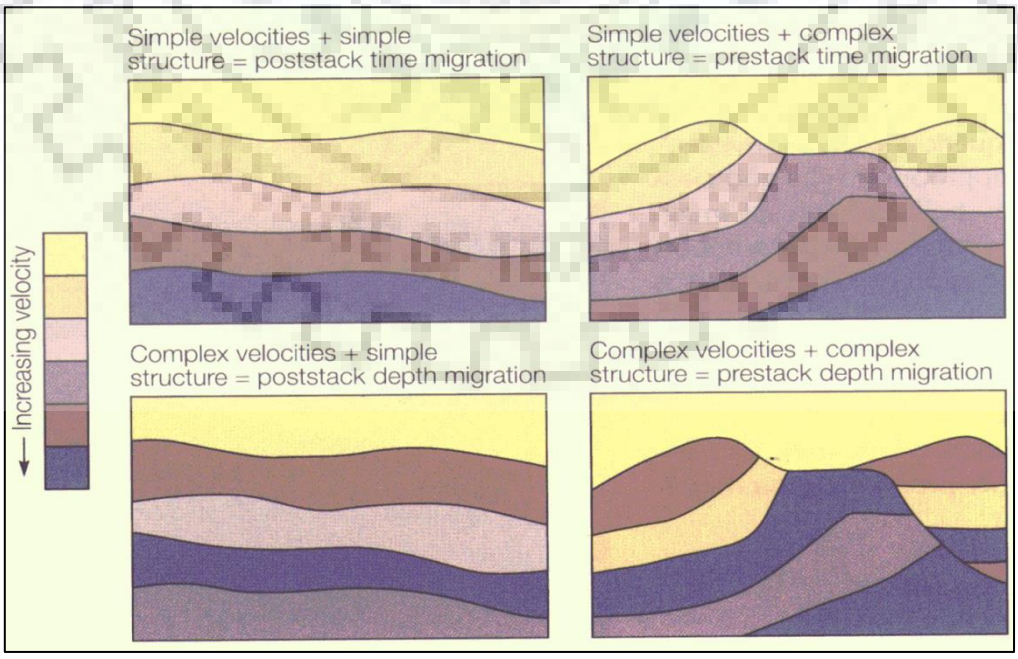


**Figure 3.2.30: Factors deciding choice of migration technique (Yilmaz, 2001).**

Migration may be applied before or after stacking. Post-stack migration is computationally less intensive compared to pre-stack migration, but requires dip-moveout correction as a prerequisite, while latter does not. Both involve creating an apparent common reflection- point gather (Fig.3.2.29 (c)) using the CMP-gathers in order to remove the reflection point smear (Fig.3.2.29 (b)).

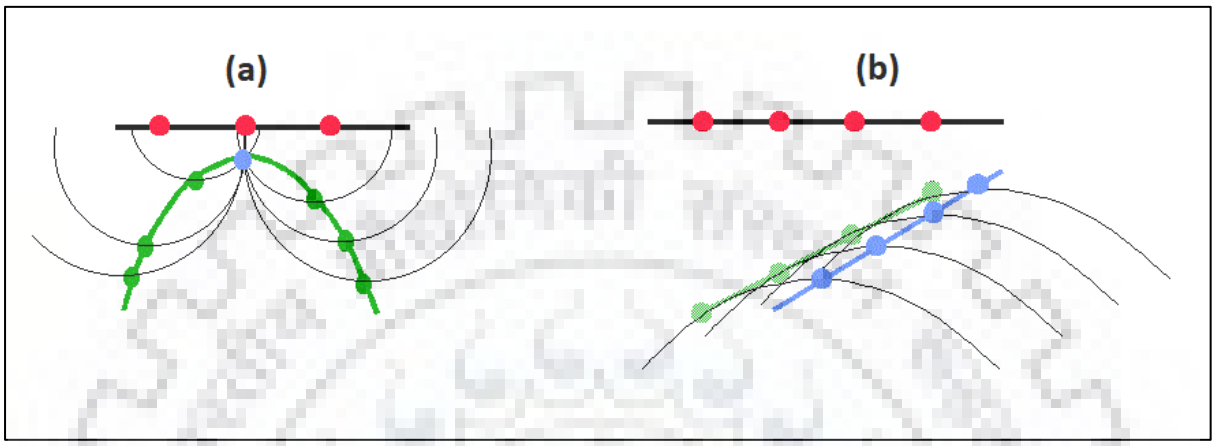


**Figure 3.2.31: Migration of a diffraction hyperbola (a) and a dipping reflector (b) (Source - http://bit.do/eSpPg).**

From the previously generated stacked images (Fig.3.1.15 & Fig.3.2.27), we could say that the profile has dipping reflectors i.e. not an ideal structure. The stacking velocities picked during velocity analysis increase with depth and show no abnormal characteristics i.e. there is a simple velocity structure. Now given that the region has dipping reflectors and simple velocity structure, we choose to use pre-stack time migration (Fig.3.2.30).

Migration traces the wave paths using the wave equation to reconstruct the wave-field at every space & time co-ordinate (Fig.3.2.31). RMS velocity section & CMP-gather are required as inputs for performing pre-stack migration. The RMS velocities are calculated (Fig.3.2.32) using the previously picked stacking velocities. Kirchhoff pre-stack time migration was performed (Fig.3.2.33 (a)) using this newly created RMS velocity section and the previously de-ghosted CMP-gathers (Fig.3.2.33 (b)).

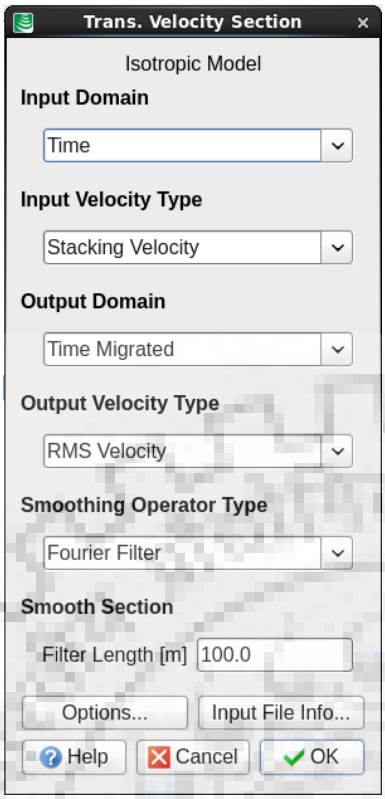


**Figure 3.2.32: Estimating RMS velocity from stacking velocity (Source - Paradigm).**

After completing pre-stack migration, Paradigm automatically stacks the migrated gathers using the same input velocities and generates a stacked section as shown in figure (3.2.34). Migration generally steepens the dipping events (Fig.3.2.31 (a)) and also collapses any diffraction hyperbolas present (Fig3.2.31 (b)). A migration process not performed in 3D is an incomplete process and as a result, the out-of-plane reflections would remain in data.

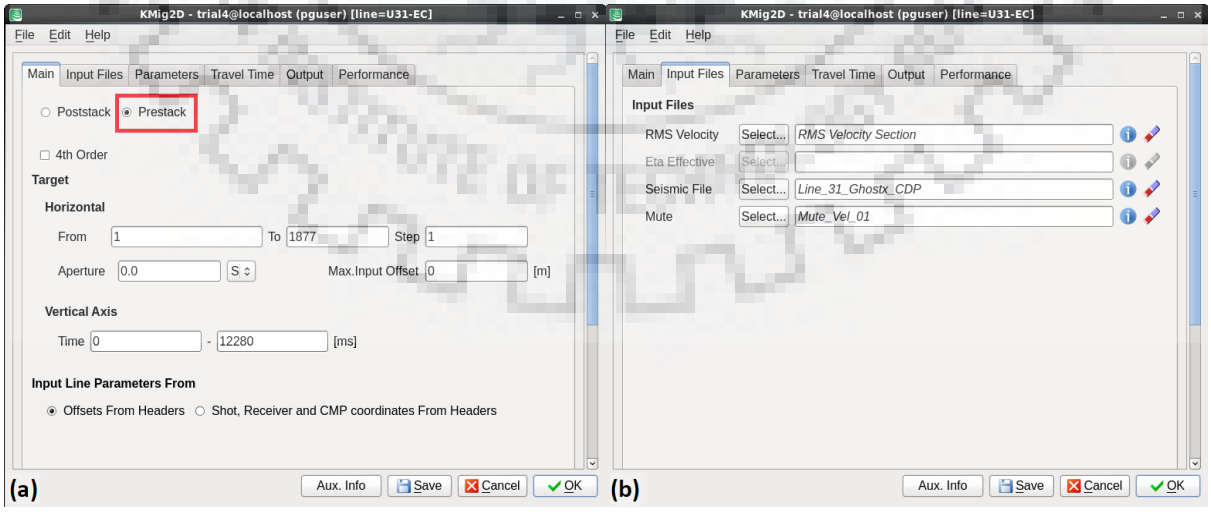


**Figure 3.2.33: (a) Pre-stack time migration (PSTM) window; (b) Input files for performing PSTM (Source – Paradigm).**

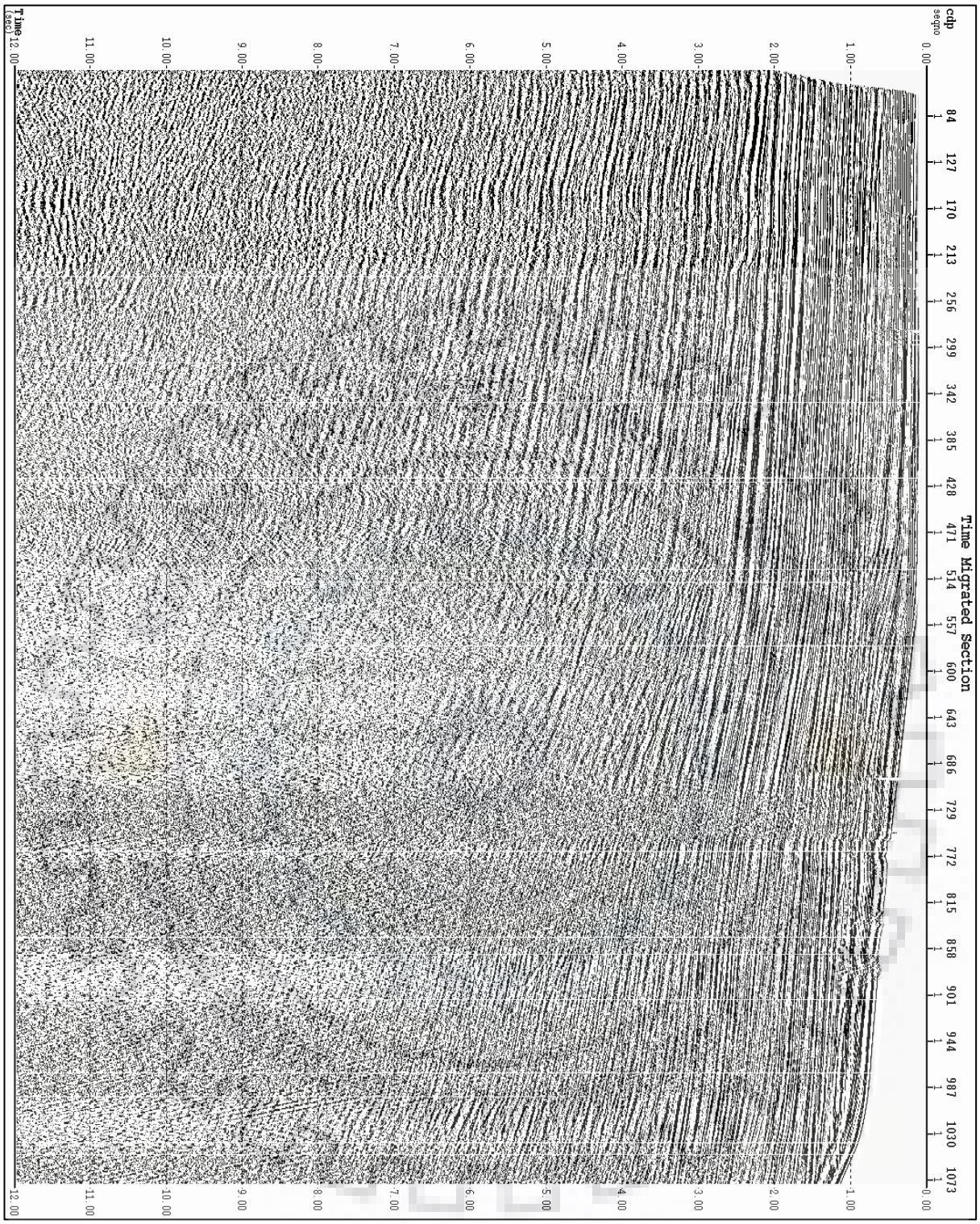


**Figure 3.2.34: Stacked section generated after pre-stack time migration.**

# 3.3. POST-PROCESSING

Migrated stack could be further conditioned by suppressing the remaining noise without disturbing primary reflections. The objective of post-processing is to achieve this and to ultimately create a clearer image of subsurface. Within Paradigm, we have used the following workflow of modules as shown in figure (3.3.1):

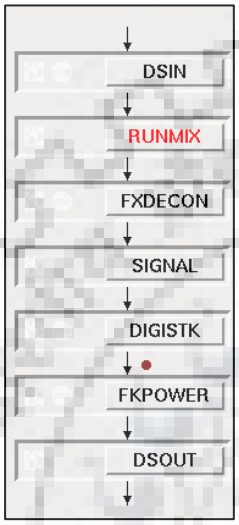


**Figure 3.3.1: Workflow of post-processing (Source - Paradigm).**

The first module in the workflow, the “RUNMIX” module is used to perform a running mix of seismic traces, using either mean or median method, and outputs a mixed trace system for further processing. The user can choose the method and number of traces used for calculating the mixed traces (Fig.3.3.2).

```
9          NTRACES - Number of traces in filter to MIX (must be odd)
ACROSS     ENSSW   - Mix within or across records (WITHIN/ACROSS)
MEDIAN     METHOD  - Method used to compute output trace amplitudes (MEAN/MEDIAN)
           HDRNAM  - Header name
```

**Figure 3.3.2: The input parameters of “RUNMIX” module (Source - Paradigm).**

```
21         XLEN    - Width of window for FFT (# traces)
161        TLEN    - Time length of window for FFT (ms)
           NFPTS   - Filter length (# spatial points)
1          NITER   - Number of predictive operation iterations
0          FLOW    - Low frequency to transform
           FHIGH   - High frequency to transform
```

**Figure 3.3.3: The input parameters of “FXDECON” module (Source - Paradigm).**

Applying a post-stack deconvolution is a common practice for removing remaining short period multiples. We have used the “FXDECON” module to perform such a

deconvolution. In order to enhance the signal it starts by transforming a given number of time samples i.e. “TLEN” within a given number of traces i.e. “XLEN” (Fig.3.3.3) into Fourier-space (*f* – *x*) domain, using fast Fourier transform to transform algorithm. An independent analysis is performed for each frequency component to create a spatial deconvolution filter for enhancing the primary energy. Note that a unique filter is constructed for each frequency and that the filters are complex, with real and imaginary coefficients.

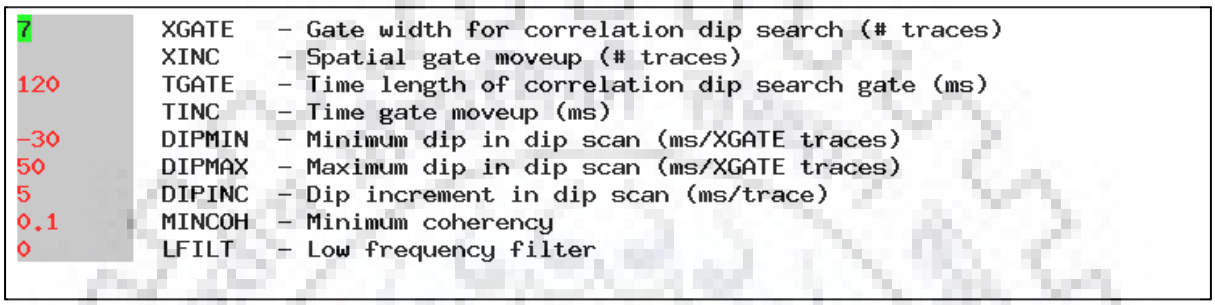


**Figure 3.3.4: The input parameters of “SIGNAL” module (Source - Paradigm).**

A combination of “SIGNAL” and “DIGISTK” modules is used to supress remaining coherent noise. The “SIGNAL” module (Fig.3.3.4) compares samples within a window to identify events with a minimum specified coherency and a dip falling within a given range in order to generate a series of signal traces. The “DIGISTK” module stacks these signal traces with the original ones. The only parameter supplied is the relative weight “WT” given to the signal traces. A negative weight can be used to rid the data of coherent noise.

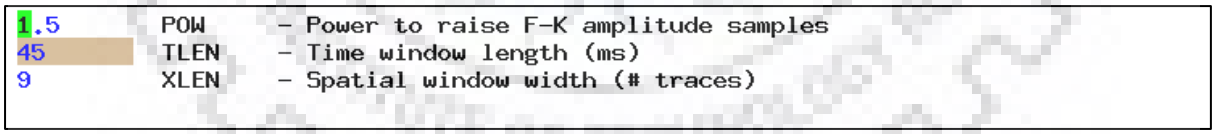


**Figure 3.3.5: The input parameters of “FKPOWER” module (Source - Paradigm).**

A “FKPOWER” module is used to enhance the signal power in a window of seismic data by first performing a multichannel time-variant $f - k$ transform and then increasing the amplitude of every sample to a minimum specified limit “POW” (Fig.3.3.5). Finally an inverse transform is applied to transform data back into time-space domain. The resulting data has much lower amplitude of random noise within data. The resultant stack after the post processing is shown by figure (3.3.6).

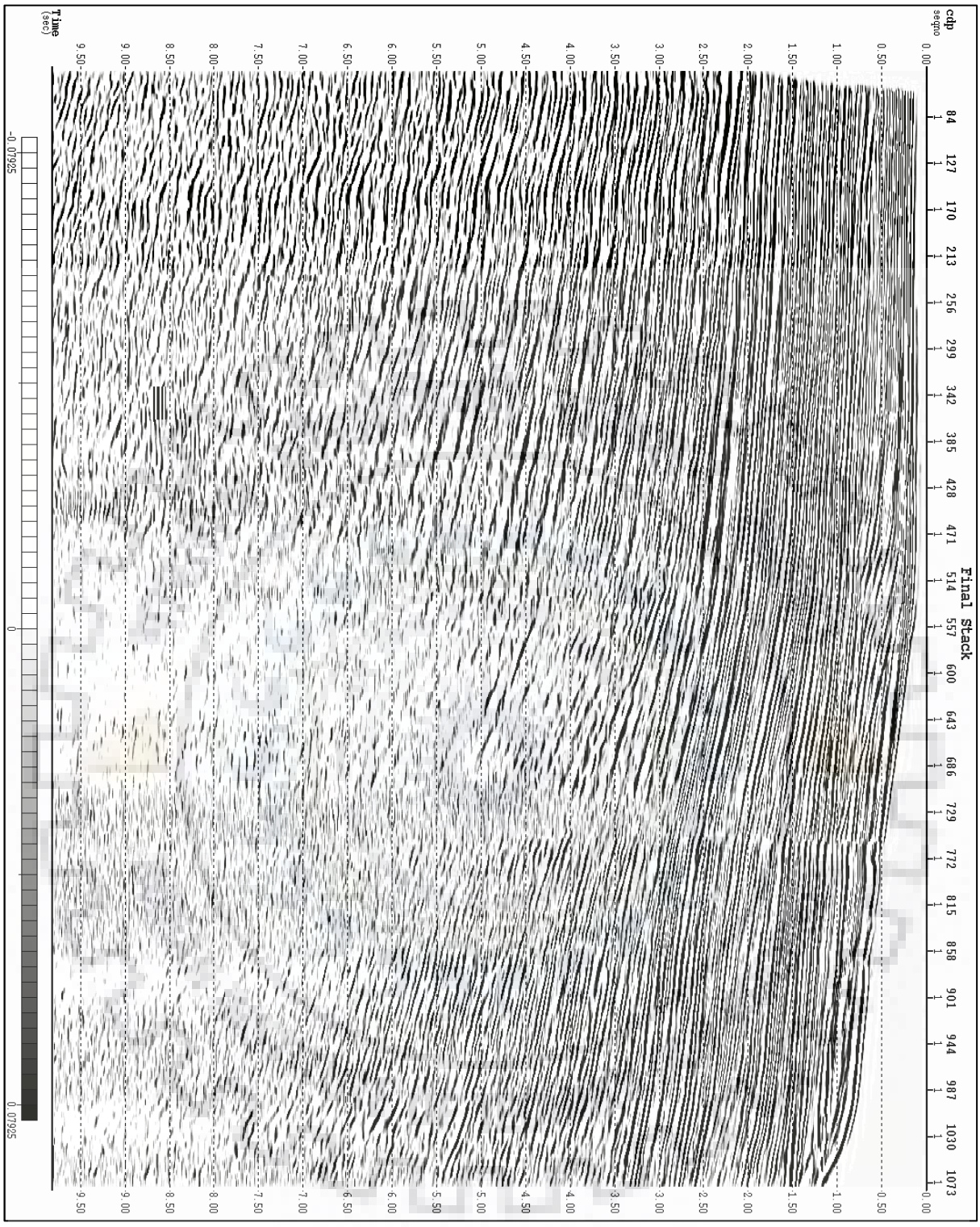


**Figure 3.3.6: Stacked image of line 31 after post-processing.**

# 4. RESULTS & DISCUSSION

Here we would study the final migrated and stacked images of all the profiles i.e. lines 30, 31 and 32. The main aim of the study was to identify geological structures and study the seismic stratigraphy of the shelf region. The fact that these profiles are perpendicular to strike direction enable us see maximum variation. We have marked the major visible horizons in red in all the studied sections.

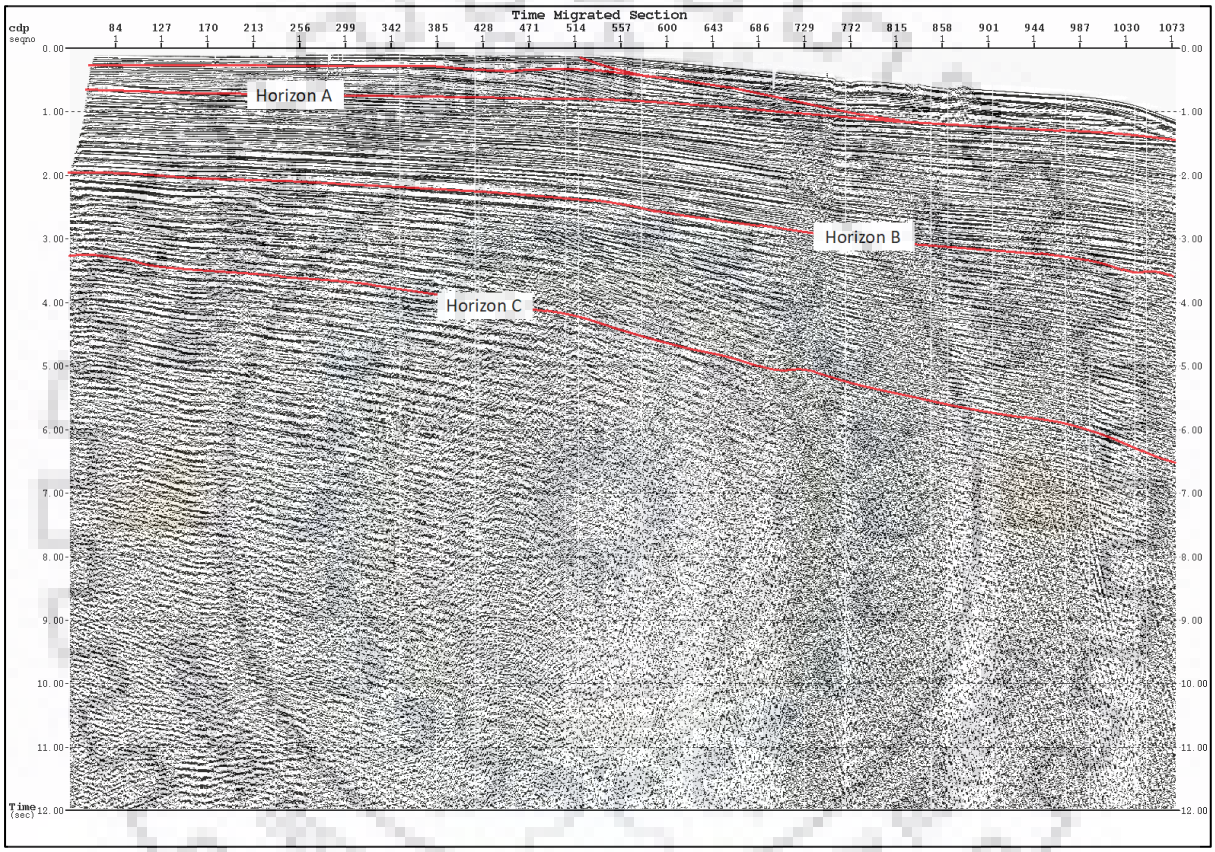


**Figure 4.1.1: Migrated and stacked seismic cross-section of line 31.**

Before we start we would take a look at some problems associated with shallow water data. In shallow water, this noise interferes with the ocean-bottom and shallow sub-bottom reflections; as a result muting might remove the ocean-bottom and shallow reflections from the final stacked data. Muting is a pre-stack processing procedure that removes noise, such as shallow refractions or normal-moveout (NMO) stretch, from CMP-gathers by zeroing amplitudes. Careful muting can minimize the effect, but some data are invariably lost along profiles, especially where the geometry of acquisition causes the near-offset to be several times longer than

the water depth. The mutes typically affect ocean bottom reflections but the deeper reflections are unaffected.

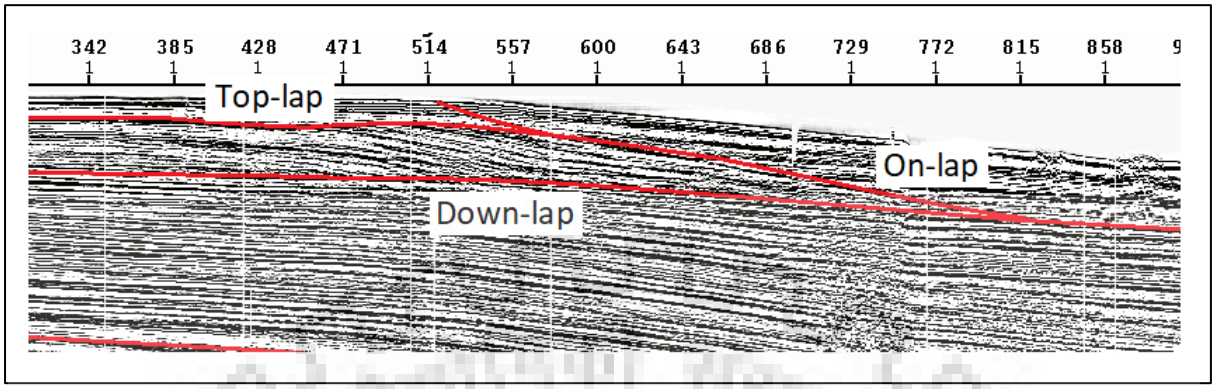


**Figure 4.1.2: Zoomed-in image of line 31.**

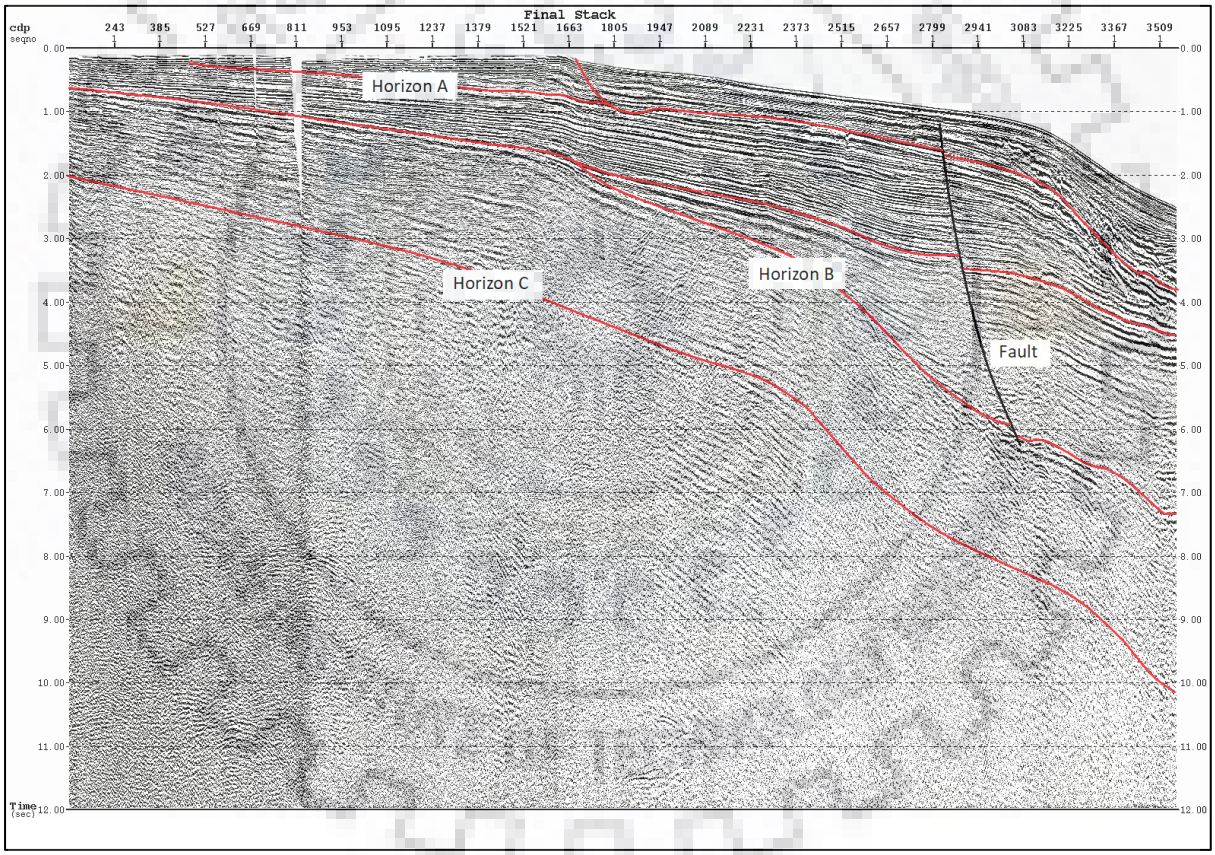


**Figure 4.1.3: Migrated and stacked seismic cross-section of line 32.**

First we discuss the profile of line 31 as shown in figure (4.1.1). The region has thick sediment cover throughout. We have identified three major horizons across all three profiles and we have labelled them horizon A, B and C. There are also many minor reflectors in between. The horizons are dipping seawards and the amount of dip increases with depth, a trend seen in all profiles. Columns of low amplitudes can be

seen in the profile, which resembles the gas chimney effect. This may be indicative of a possible gas deposit in the region. The profile also shows us a classic example of top-lap, down-lap and on-lap as seen in figure (4.1.2), which shows a zoomed part of line 31's profile. This is suggestive of eustatic i.e. sea-level changes, with top and down-laps corresponding to regression i.e. seaward movement of shoreline and on-lap corresponding to transgression i.e. landward movement of shoreline.

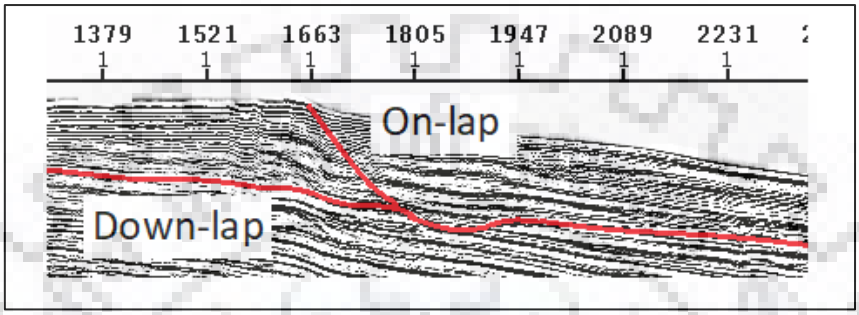


**Figure 4.1.4: Zoomed-in image of line 32.**

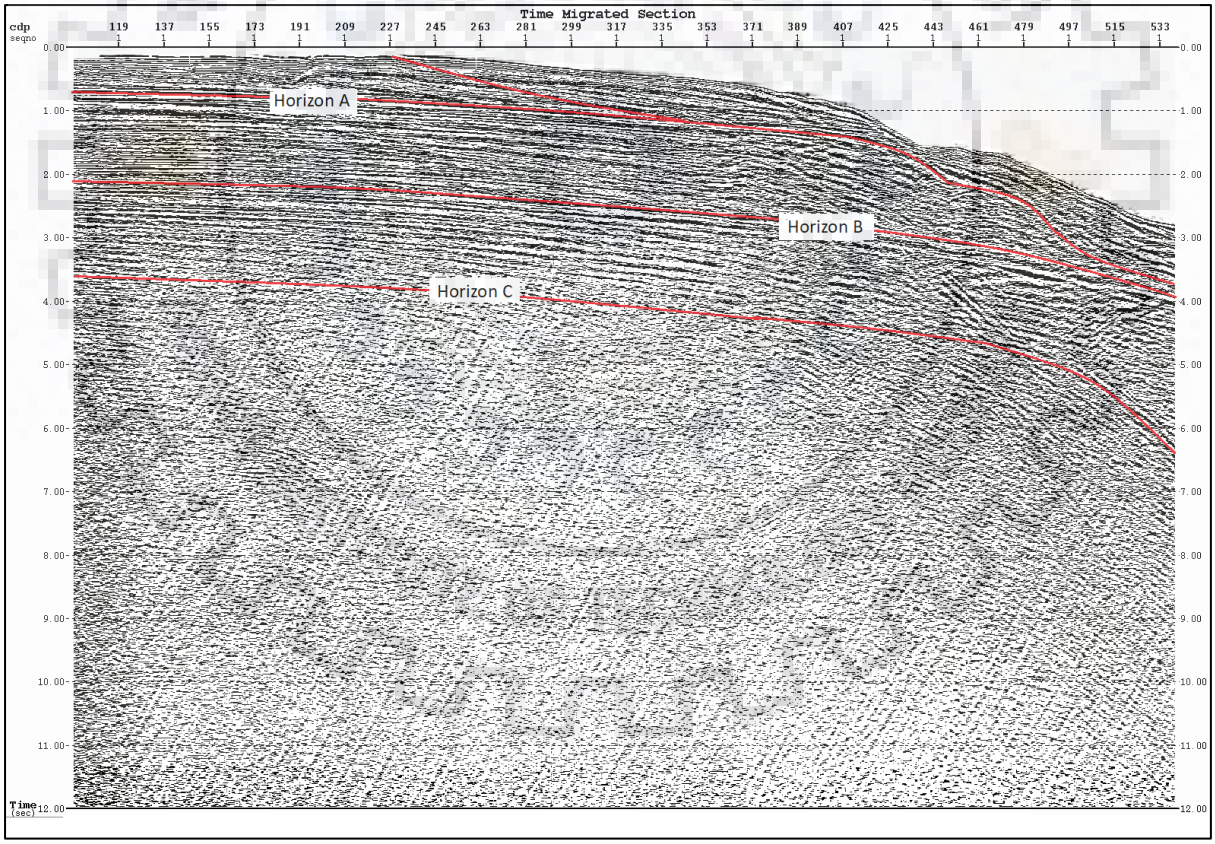


**Figure 4.1.5: Migrated and stacked seismic cross-section of line 30.**

Figure (4.1.2) shows seismic profile of line 32, which by far has most complex structure of the three profiles studied. The previously mentioned horizons A, B and C are also visible here and all of them have a seaward dip. Again the amount of dip

increases with depth; however, the amount of dip is considerably more compared to the profile of line 31. A major normal fault is also visible in the section. Such a trap may house a possible oil & gas deposit. Like line 31 a down-lap and an on-lap are also visible here (Fig.4.1.4), providing more evidence for the eustatic changes.

Profile of line 30 is the simplest one with almost horizontal reflectors (Fig.4.1.5), dipping very slightly seawards. Their dips, more or less remain constant with depth. The peculiar on-lap and down-lap pair is visible here as well. The data quality is quite poor below the horizon C, hence, no discernible major reflector is visible.

# 5. REFERENCES


- Yilmaz O., 2001, Seismic Data Analysis: Processing, Inversion and Interpretation of Seismic Data: SEG.
- Telford W. M. , Geldart L. P. , Sheriff R.E., 1993, Applied Geophysics (second edition): Cambridge University Press.
- Reynolds J.M., 1997, An introduction to applied and environmental geophysics: Chichester, John Wiley.
- Upadhyay, S.K., 2004, Seismic Reflection Processing. Springer, Berlin, Heidelberg.
- Dillon, W.P., Paull, CK., and Gilbert L.E., 1985, History of the Atlantic Continental Margin off Florida; The Blake Plateau basin, in Poag, C.W., ed., Geologic evolution of the United States Atlantic margin: New York, Van Nostrand Reinhold, p. 189-215.
- Dillon, W.P., and Popenoe, P., 1988, The Blake Plateau Basin and Carolina Trough, in Sheridan, R.E., and Grow, J.A., eds., The Atlantic Continental Margin, U.S.: Geological Society of America, The Geology of North America, v. 1-2, p. 291 - 328.
- Dillon, W.P., Popenoe, P., Grow, J.A., Klitgord, K.D., Swift, B.A., Paull, C.K. and Cashman, K.V., 1983, Growth faulting and salt diapirism, their relationships and control in the Carolina Trough, eastern North America, in Watkins, J.S., and Drake, C.L., eds., Studies in continental margin geology: American Association of Petroleum Geologists Memoir 34, p. 21-46.
- Dix, C.H., 1955, Seismic velocities from surface measurements: Geophysics, v. 20, p. 68-86. Dowling, J.J., 1968, The East Coast onshore-offshore experiment, II. Seismic refraction measurements on the continental shelf between Cape Hatteras and Cape Fear: Bulletin of the Seismological Society of America, v. 58, p. 821 - 834.
- Hutchinson, D.R., Grow, J.A., Klitgord, K.D., and Swift, B.A., 1983, Deep structure and evolution of the Carolina Trough, in Watkins, J.S., and Drake, C.L., eds., Studies in Continental Margin Geology: American Association Petroleum Geologists Memoir 34, p. 129-152.

- Klitgord, K.D., and Behrendt, J.C., 1979, Basin structure of the U. S. Atlantic margin: American Association Petroleum Geologists Memoir 29, p. 85-112.
- NOS (National Ocean Service), 1986, Bathymetric Map of the Atlantic Ocean, southeastern United States: Washington (U.S. Department of Commerce, National Oceanic and Atmospheric Administration), 1:1,000,000.
- Poag, C.W., 1991, Rise and demise of the Bahama-Grand Banks gigaplatform, northern margin of the Jurassic proto-Atlantic seaway, Marine Geology, 102, p. 63-130.
- Sheridan, R.E., and Enos, P., 1979, Stratigraphic evolution of the Blake Plateau after a decade of scientific drilling, in Talwani, M., Hay, W., and Ryan, W.B.F., eds., Deep drilling results in the Atlantic Ocean: Continental margins and paleoenvironment: Maurice Ewing Series, v. 3, American Geophysical Union Geophysical Monograph, p. 109-122.